ELSEVIER

Contents lists available at ScienceDirect

#### Bioorganic & Medicinal Chemistry

journal homepage: www.elsevier.com/locate/bmc





# Targeting fungal biofilms: design, synthesis, biological and in silico studies of novel N-(5-undecyl-1,3,4-oxadiazol-2-yl)benzamide derivatives against Candida albicans

A.C. Kumar<sup>a</sup>, Madalambika<sup>a</sup>, P.M. Bharathkumar<sup>a</sup>, Priyanka R. Patil<sup>a</sup>, J. Rangaswamy<sup>b</sup>, Ramith Ramu<sup>c</sup>, K.B. Vilas Gowda<sup>c</sup>, Nagaraja Naik<sup>a,\*</sup>

- <sup>a</sup> Department of Studies in Chemistry, Manasagangotri, University of Mysore, 570006, Karnataka, India
- <sup>b</sup> Department of Chemistry, Poornaprajna College, Shree Adamaru Matha Education Council, Mangalore University, Karnataka, India
- <sup>c</sup> Department of Biotechnology and Bioinformatics, JSS Academy of Higher Education and Research, Mysore 570015, Karnataka, India

#### ARTICLE INFO

# Keywords: 5-Undecyl-1,3,4-Oxadiazole-2-benzamide Candida albicans Biofilm inhibition Filament inhibition Hemolysis Cytotoxicity SAR studies Molecular docking ADMET

#### ABSTRACT

The inhibition of fungal biofilm formation has garnered significant attention as a promising therapeutic strategy against fungal infections. In this study, a series of N-(5-undecyl-1,3,4-oxadiazol-2-yl)benzamide derivatives 5 (a-o) were synthesized as novel biofilm inhibitors targeting Candida albicans, utilizing the well-known biological activities linked with the oxadiazole nucleus. The in vitro antifungal activity of all derivatives was evaluated using the broth microdilution method, with fluconazole serving as the reference drug. Notably, compound 5e exhibited potent activity, with a minimum inhibitory concentration (MIC) of 7 µg/mL and a minimum fungicidal concentration (MFC) of 32 µg/mL, outperforming the standard drug (MIC: 8 µg/mL; MFC: 64 µg/mL). Biofilm and hyphal filament inhibition assays further revealed that compound 5e achieved 86.29 % inhibition of biofilm formation and 72.30 % inhibition of fungal filamentation. Additionally, RT-PCR analysis demonstrated that treatment with compound 5e significantly downregulated the expression of key biofilm genes, including ALS1, ALS3, and HWP1. Scanning electron microscopy (SEM) of C. albicans treated with 5e confirmed substantial inhibition of biofilm formation compared to both untreated controls and the fluconazole-treated group. Screening of compound 5e for blood compatibility by hemolytic assay revealed 4.83 % cell lysis at 1125 µg/mL, and cytotoxicity assay on human HEK293 cell line demonstrated that compound 5e was non-toxic to normal cells at the tested concentrations. Furthermore, molecular docking studies to investigate the potential binding interactions of the lead compound, along with ADMET analysis, were performed to assess pharmacokinetic and bioavailability profiles. The enhanced bioactivity of compound 5e is associated with the presence of an orthosubstituted hydroxy group, a 1,3,4-oxadiazole core, and a long hydrophobic alkyl chain, which collectively improve target binding, membrane interaction, and antifungal effectiveness. These findings suggest that compound 5e is a promising candidate for the development of next-generation antifungal agents to combat drugresistant Candida albicans infections.

#### 1. Introduction

Candida species generally exist as harmless organisms, mainly inhabiting mucosal surfaces of the gastrointestinal, urogenital, and respiratory tracts. The genus *Candida* includes several opportunistic yeast species, with *Candida albicans* being the most common and versatile fungal pathogen that typically causes superficial, easily treatable infections. Although usually a harmless resident of mucosal surfaces, *C. albicans* can become invasive when immunity is suppressed or when

antibiotics disrupt the normal microbial balance.3,4 It is notably one of the most common causes of bloodstream infections acquired in health-care settings.5 Since it can invade the bloodstream, leading to deeptissue infections under favourable conditions, it is often associated with high morbidity and mortality.6–8 A key feature of *C. albicans* virulence is its ability to switch between yeast and hyphal forms.9 This morphological change is essential for tissue invasion and biofilm development. Biofilm is a complex community of microbes attached to surfaces and encased in a protective matrix of exopolysaccharides,

E-mail address: drnaikchem@gmail.com (N. Naik).

<sup>\*</sup> Corresponding author.

which shields the microbial cells and promotes colonization. 10,11 Biofilms contribute to resistance against antifungal treatments and increase pathogenicity, making them 30-2000 times more resistant than yeast.12,13 At a molecular level, the formation of biofilms and hyphal growth is regulated by a network of signalling pathways and transcription factors that control the expression of key adhesins and virulence factors.14,15 Genes such as ALS1, ALS3, ECE1, HGC1, HWP1, HYR1, RBT1, RBT4, and UME6 produce surface proteins that assist the fungus in sticking to host tissues and promote hyphal filament growth.16-18 The ALS gene family, particularly ALS1 and ALS3, along with HWP1, is crucial for cell-to-cell adhesion and biofilm stability, and these are regulated by transcription factors Tor1, Efg1, and Bcr1.19,20 These genetic networks coordinate the morphological changes necessary for virulence. The increasing rates of antifungal resistance and the rising minimum inhibitory concentrations (MICs) for major antifungal classes, including azoles, amphotericin B, and echinocandins in various Candida species, emphasize the urgent need for molecular insights that can guide the development of new therapies targeting virulence mechanisms, biofilm formation, or adhesion processes.21

To date, azole antifungals remain the most commonly used medications for treating fungal infections.22 Among them, fluconazole, voriconazole, itraconazole, and posaconazole play key roles in managing invasive fungal infections (Fig. 1). While generally well tolerated, these agents are known to inhibit cytochrome P450 enzymes, leading to potential drug–drug interactions.23–25 Additionally, the need for high dosages often results in adverse side effects and contributes to the development of drug resistance.26,27 In this context, heterocyclic compounds have gained prominence as scaffolds for drug discovery due to their structural versatility and bioactivity.28

Among these heterocyclic compounds, 1,3,4-oxadiazole derivatives have emerged as a privileged class, exhibiting a wide range of pharmacological activities, including antimicrobial, anticancer, anti-inflammatory, and antifungal effects.29–31 Also, 1,3,4-oxadiazoles are believed to inhibit fungal thioredoxin reductase, an enzyme crucial for fungal cell survival.32–35 The 1,3,4-oxadiazole ring is a five-membered structure containing two nitrogen atoms and one oxygen atom, which enhances electron delocalization, lipophilicity, and hydrogen bonding potential. When coupled with a benzamide moiety, the resulting 1,3,4-oxadiazole-2-yl-benzamide derivatives offer enhanced bioactivity due to greater molecular rigidity and improved interaction with fungal targets.36,37

According to recent research, the antifungal effectiveness is greatly influenced by the substitution pattern on the benzamide core and

oxadiazole ring.38 The potential of this scaffold in the logical development of next-generation antifungal medicines is demonstrated by these structure—activity relationships (SAR).

Several conventional drugs containing 1,3,4-oxadiazoles are available on the market (Fig. 2) to treat various diseases. Considering the therapeutic significance of oxadiazole scaffolds and our interest in synthesizing 1,3,4-oxadiazoles,39 herein, we present the synthesis of a series of 1,3,4-oxadiazole-based benzamide derivatives to explore their potential to inhibit biofilm formation against *Candida albicans* and to study their physicochemical properties. (See Fig. 3)

Although oxadiazoles are well-established antifungal scaffolds, our derivatives incorporate a long alkyl substituent derived from lauric acid, which has not been systematically explored before. Lauric acid was selected as a starting material due to its long lipophilic side chain, providing an amphiphilic scaffold favourable for drug design, which can enhance membrane permeability and facilitate both hydrophobic and hydrophilic interactions with biological targets. 40,41 Conversion of lauric acid into its heterocyclic derivative, 1,3,4-oxadiazole-2-amine, followed by acid-amine coupling with variously substituted aromatic carboxylic acids, offers a rational approach for generating novel bioactive molecules with improved therapeutic potential. This modification was specifically designed to enhance lipophilic interactions with fungal membranes and active site hydrophobic pockets, improving antifungal potency and selectivity. The novelty of our approach lies in tailoring the oxadiazole core with extended hydrophobic chains, providing new structure-activity relationship insights and distinguishing these derivatives from conventional oxadiazoles reported in the literature.

#### 2. Results and discussion

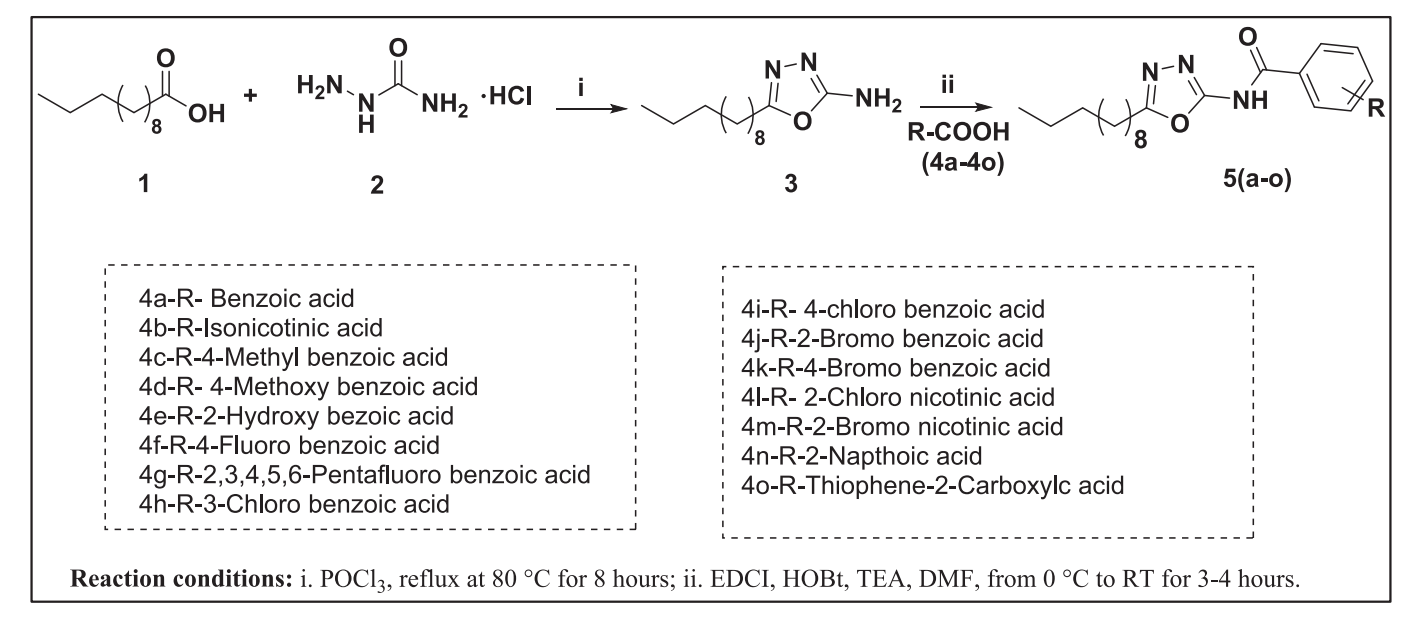
#### 2.1. Chemistry

New N-(5-undecyl-1,3,4-oxadiazol-2-yl)benzamide derivatives **5(a-o)** were synthesized by two-step synthetic route. In the first step, a stoichiometric amount of lauric acid **(1)** and semi carbazide hydrochloride **(2)** reacted under refluxing phosphorus (V) chloride at 80 °C to produce 5-undecyl-1,3,4-oxadiazole-2-amine **(3)**. In the second step, compound **(3)** undergoes amide formation with various aromatic acids **4 (a-o)** using coupling reagents to yield the final compounds **5(a-o)**. All synthesized compounds were extracted and purified via column chromatography to obtain pure products in good yields (Scheme 1). The compounds were characterized using <sup>1</sup>H NMR, <sup>13</sup>C NMR, and LC-MS techniques. The 5-undecyl-1,3,4-oxadiazole-2-benzamide derivatives **5** 

Fig. 1. Commercially available azole-containing antifungal drugs.

Fig. 2. Conventional drug containing 1,3,4-oxadiazole nucleus.

Fig. 3. N-(5-undecyl-1,3,4-oxadiazol-2-yl)benzamide derivatives 5(a-o) with % yield.



Scheme 1. Systematic route for the synthesis of N-5-undecyl-1,3,4-oxadiazol-2-yl)benzamide derivatives 5(a-o).

(a-o) were confirmed by the appearance of characteristic peaks at downfield regions for aliphatic protons from  $\delta$  0.8 to 2.9 ppm, a singlet peak resonated at  $\delta$  5.5 to 6.8 ppm attributed to the -NH proton of the amide by the disappearance of peak at  $\delta$  11–12 ppm corresponding to carboxylic acid (-COOH), and presence characteristic aromatic peaks at  $\delta$  ~6.8 to ~7.8 ppm in the  $^1{\rm H}$  NMR spectrum, indicating the formation of the expected product. The presence of all necessary peaks and the absence of extraneous signals in both  $^1{\rm H}$  and  $^{13}{\rm C}$  NMR spectra confirm the structures. Additionally, the mass spectra obtained were consistent with the assigned structures.

#### 2.2. Biological studies

# 2.2.1. Evaluation of antifungal activities by broth microdilution (BMD) method

The antifungal activity of the synthesized compounds 5(a-o) was evaluated against Candida albicans by the BMD method for determining their Minimum Inhibitory Concentration (MIC) and Minimum Fungicidal Concentration (MFC), with fluconazole (FLC) as the standard reference drug. As illustrated in Fig. 4 and Fig. 5, FLC demonstrated an MIC of approximately 8 µg/mL, consistent with its established inhibitory profile. Among the tested compounds, 5e exhibited the lowest MIC of 7 μg/mL, indicating the highest antifungal potency. Compounds 5a, 5j, 5 k, 5 l, 5 m, and 50 showed MIC values between 9 and 12  $\mu g/mL$ , suggesting notable antifungal activity. Conversely, 5f and 5 g demonstrated the highest MICs (14  $\mu$ g/mL and 18  $\mu$ g/mL), reflecting lower inhibitory effects. In terms of fungicidal activity (Fig. 5, right panel), Compound 5e showed the lowest MFC of 32 µg/mL, outperforming FLC and indicating a strong fungicidal effect, whereas FLC presented an MFC of 64 ug/mL. The compound **5b** exhibited an MFC of 64 µg/mL, and compounds 5c, 5d, 5i, 5j, 5l, 5 m, and 5o showed intermediate MFC values of 128 µg/ mL, reflecting moderate fungicidal efficacy. Notably, 5a, 5f, 5g, 5h, 5k, and 5n displayed a high MFC of 256 µg/mL, correlating with its elevated MIC, and further supporting its weaker antifungal performance.

Experiments were conducted in triplicate, and values are represented as mean  $\pm$  SD. Error bars indicate standard deviations. Statistical analysis was performed using Student's *t*-test with Bonferroni correction for multiple comparisons. \*p < 0.05, \*\*p < 0.01, \*\*p < 0.001 compared to fluconazole (FLC).

#### 2.2.2. Biofilm inhibition assay

The antibiofilm activity of the synthesized compounds **5(a-o)** was evaluated against *Candida albicans* and compared with the standard antifungal agent FLC by the crystal violet quantification method. The results revealed that the standard drug fluconazole exhibited 76.5 % inhibition of biofilm formation, whereas 2-hydroxy-N-(5-undecyl-1,3,4-oxadiazol-2-yl)benzamide (**5e**) demonstrated **86.29** % biofilm inhibition, surpassing FLC and indicating potent antibiofilm activity. In contrast, the other compounds **5b**, **5 m**, and **5o** showed substantial inhibition of **51.2** %, **57.4** %, and **59.0** % inhibition, respectively (Fig. 6). Further moderate antibiofilm activity, ranging between 42 and 49.4 %, was observed for compounds **5a**, **5c**, **5 h**, **5 k**, **5 l**, **and 5n**. The

remaining compounds, such as **5d**, **5f**, **5g**, **5i**, and **5j**, displayed relatively lower inhibition levels in the range of 29.5–39.5 %, suggesting weaker antibiofilm properties (results are presented in Fig. 7 and Table 1. Overall, these results highlight **5e** as the most effective candidate for inhibiting *C. albicans* biofilm formation, and **5b**, **5 m**, and **5o** also demonstrated promising activity suitable for further investigation in antifungal strategies targeting biofilm-associated infections.

#### 2.2.3. Filament inhibition assay

The filament inhibition assay against *C. albicans* revealed differential inhibitory effects among the tested compounds. The study revealed that compound **5e** exhibited the highest filament inhibition of **72.3** %, in comparison to FLC, which showed 60 % inhibition, indicating strong anti-filamentation potential. Compounds **5b**, **5 l**, **and 5o** also demonstrated considerable inhibition, ranging from **49.8 to 52.3** % (**Fig. 8**), followed by 5f, 5d, 5 h, 5 k, 5 m, and 5n, which showed significant inhibition in the range of 37 % to 43.8 %. In contrast, compounds **5a**, **5c**, **5** g, **5i**, and **5j** displayed moderate inhibitory activity ranging between 23 % and 34.7 %, suggesting limited effectiveness in suppressing hyphal formation. These findings highlight compound **5e** as the most promising antifungal candidate among the tested derivatives, with superior efficacy in inhibiting filamentation, a key virulence factor in *C. albicans*. This suggests its potential as an effective lead compound in antifungal drug development. The results are represented in **Fig. 9** and **Table 1**.

Experiments were conducted in triplicate, and values are represented as mean  $\pm$  SD. Error bars indicate standard deviations. Statistical analysis was performed using Student's *t*-test with Bonferroni correction for multiple comparisons. \*p < 0.05, \*\*p < 0.01, \*\*p < 0.001 compared to fluconazole (FLC).

#### 2.2.4. Analysis of C. albicans biofilm gene expression using RT-PCR

Quantitative real-time PCR analysis demonstrated that treatment with fluconazole (FLC) and the key lead compound 5e significantly downregulated the expression of key virulence genes HWP1, EFG1, and ALS3 in Candida albicans compared to the untreated control group. The control group exhibited the highest normalized relative quantification (NRQ) levels for all three genes, *EFG1* showing NRQ values of nearly 1.8, and HWP1 and ALS3 at approximately 1.7. Treatment with FLC reduced gene expression by about 50 %, whereas treatment with compound 5e led to even more pronounced suppression, with NRQ values falling below 0.7 for all genes assessed. These genes are integral to the pathogenicity of *C. albicans*. Specifically, *HWP1* encodes a hyphal wall protein crucial for adhesion and host interaction; *EFG1* is a central transcription factor in hyphal development regulated via the cAMP-PKA pathway; and ALS3, a member of the agglutinin-like sequence family, is involved in host tissue adherence and biofilm development. The significant downregulation of these genes, especially by compound 5e, suggests its strong inhibitory effect on hyphal formation and biofilm establishment. These findings are consistent with earlier reports that associate reduced expression of hypha-specific genes with decreased virulence and biofilm-forming capacity in C. albicans. Thus, compound 5e exhibits potential as well as a novel antifungal agent by targeting critical biofilm-

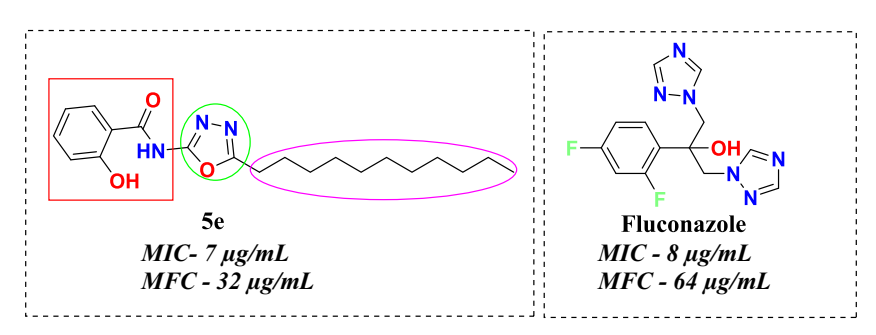


Fig. 4. MIC and MFC of compounds 5e and standard fluconazole.

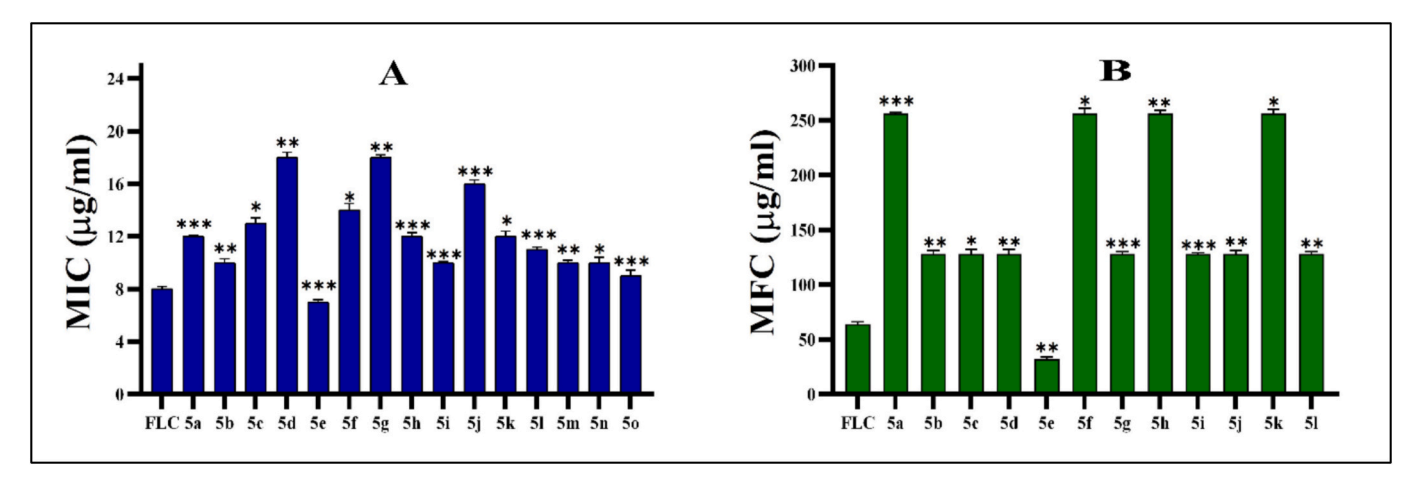


Fig. 5. A) Minimum inhibitory concentration (MIC) and B) Minimum fungicidal concentration (MFC) values of compounds 5(a-o) against *C. albicans*, with fluconazole (FLC) as the control.

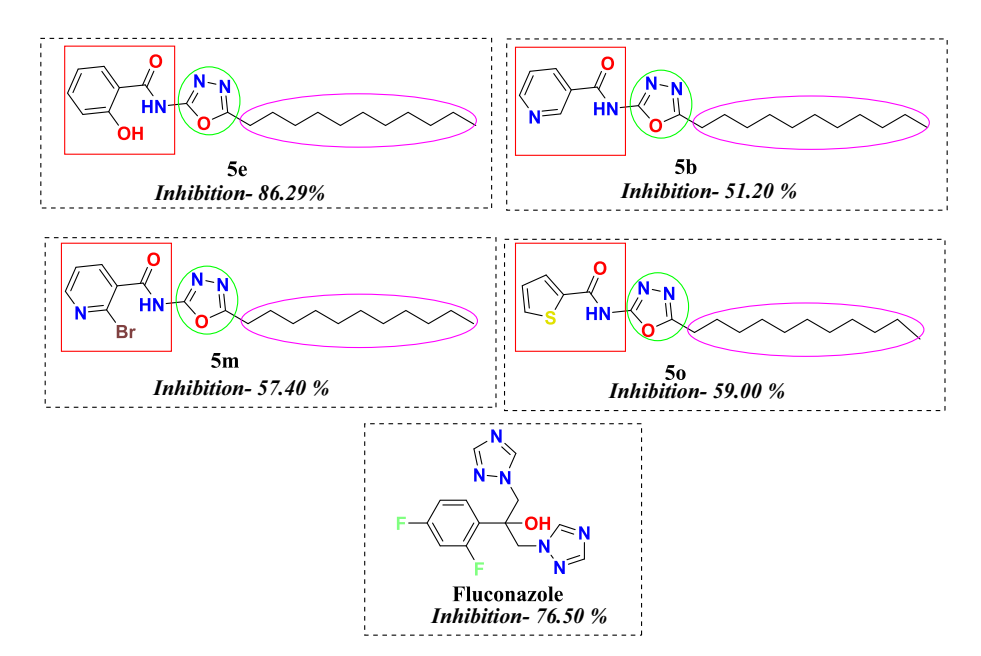


Fig. 6. % Biofilm inhibition of lead compounds and standard fluconazole.

associated genes. The results are presented in Fig. 10 and Table 2.

Expression levels were expressed as the normalized relative quantity (NRQ). Each gene expression level is normalized using the reference gene ACT1 and compared to the control. Values represent the mean  $\pm$  SD of triplicate experiments. Error bars indicate standard deviations. Statistical analysis was performed using Student's t-test with Bonferroni correction for multiple comparisons. \*p < 0.05, \*\*p < 0.01, \*\*p < 0.001 compared to fluconazole (FLC).

#### 2.2.5. Erythrocyte Hemolysis assay

The hemolytic activity of compound **5e** was assessed and compared with fluconazole across a concentration range of 1125–0.125  $\mu g/mL$ . Importantly, at the MIC,  $\frac{1}{2}\times MIC$ , and  $2\times MIC$ , as well as at the  $\frac{1}{2}\times MFC$ , MFC, and  $2\times MFC$  concentrations, **no detectable hemolysis was observed** for either compound **5e** or fluconazole, with values comparable to the saline control (p>0.05). Compound **5e** showed minimal hemolysis, with only **4.83 % cell lysis** observed at the highest tested concentration (1125  $\mu g/mL$ ). In contrast, fluconazole induced significantly higher hemolysis, with 11.0 % lysis at 1125  $\mu g/mL$  and 6.12 % lysis at 562.5  $\mu g/mL$  when compared to the compound 5e. At lower

concentrations, hemolysis by fluconazole declined in a concentration-dependent manner, as shown in Fig. 11.

#### 2.2.6. Cytotoxicity assay

The cytotoxic potential of compound **5e** and fluconazole (FLC) was assessed on HEK293 cells using the MTT assay. At the highest tested concentration (1125  $\mu g/mL$ ), compound **5e** exhibited only **8.20** % reduction in cell viability, indicating negligible cytotoxicity. In comparison, fluconazole displayed a concentration-dependent cytotoxic effect, with 6.24 % cytotoxicity observed at 562.5  $\mu g/mL$  and 14.1 % cytotoxicity at 1125  $\mu g/mL$  (Fig. 12). At all lower concentrations tested, neither compound 5e nor fluconazole caused significant loss of cell viability, with results comparable to the untreated control group (p>0.05). These findings suggest that compound 5e is minimally cytotoxic to mammalian HEK293 cells, even at concentrations far exceeding its antifungal MIC, and demonstrates a safer profile than fluconazole at comparable levels.

#### 2.2.7. SEM analysis

Scanning Electron Microscopy (SEM) was used for surface analysis,

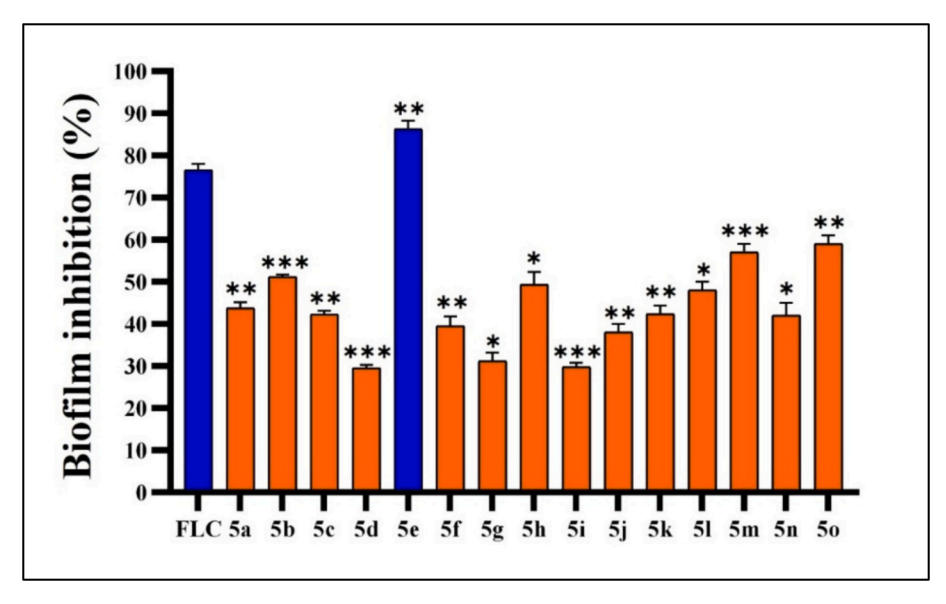


Fig. 7. Biofilm inhibition activity of compounds 5(a-o) against C. albicans, with fluconazole (FLC) serving as the control.

Table 1
Antifungal activity of synthesized compounds 5(a-o) against Candida albicans.

	, ,			
Compounds	MIC (μg/	MFC (μg/	Biofilm Inhibition	Filament
	mL)	mL)	(%)	Inhibition (%)
5a	12	256	43.8	23.4
5b	10	64	51.2	52.3
5c	13	128	42.3	26.2
5d	18	128	29.5	37
5e	7	32	86.29	72.3
5f	14	256	39.5	43.8
5g	18	128	31.2	26.2
5h	12	256	49.4	39.4
5i	10	128	29.8	34.7
5j	16	128	38.1	27.8
5k	12	256	42.4	38.9
51	11	128	48.1	49.8
5m	10	128	57.4	39.1
5n	10	256	42.9	40.1
5o	9	128	59	51.8
F LC	8	64	76.5	60

which shows the morphological features of target compounds. When the untreated *C. albicans* control group was characterized by SEM, it showed a dense and well-structured biofilm matrix, extensive hyphal networks, dense biofilm, and compact cell aggregation. In contrast, cells treated with FLC and **5e** exhibited a significant reduction in biofilm biomass

characterized by a reduction in the dense matrix of biofilm. Both treatments induced notable morphological alterations, including disrupted hyphal structures, deformed and ruptured cells, indicating delicate cell integrity and impaired biofilm development. This further confirms that the compound **5e** has potential inhibition properties of biofilm formation against antifungal activity.

#### 2.2.8. Structure-activity relationship

The antifungal evaluation of the synthesized 1,3,4-oxadiazole benzamide derivatives against Candida albicans revealed a significant correlation between structural features and biological activity. Among them, compound 5e, bearing both an ortho-hydroxyaryl group and a long lipophilic alkyl chain, exhibited the most potent antifungal activity with an MIC of 7 μg/mL. The ortho-hydroxy group likely enhances target binding through strong hydrogen bonding interactions and contributes to a stabilized bioactive conformation via intramolecular hydrogen bonding. Additionally, the presence of a long alkyl chain increases lipophilicity, which improves membrane permeability and may facilitate deeper interaction within the hydrophobic domains of the fungal enzyme active sites. Moreover, it has been shown that adding lengthy alkyl chains to the oxadiazole nucleus increases membrane permeability and compromises the integrity of fungal cells. The derivatives bearing electron-withdrawing groups like fluoro, chloro, and bromo display reduced activity, highlighting the importance of both electronic and lipophilic balance in modulating antifungal potency.

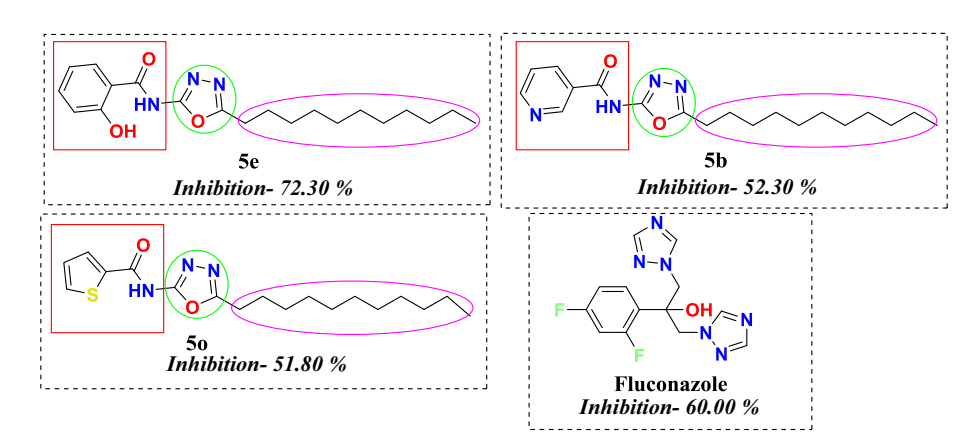


Fig. 8. % Filament inhibition of lead compounds in comparison with standard fluconazole.

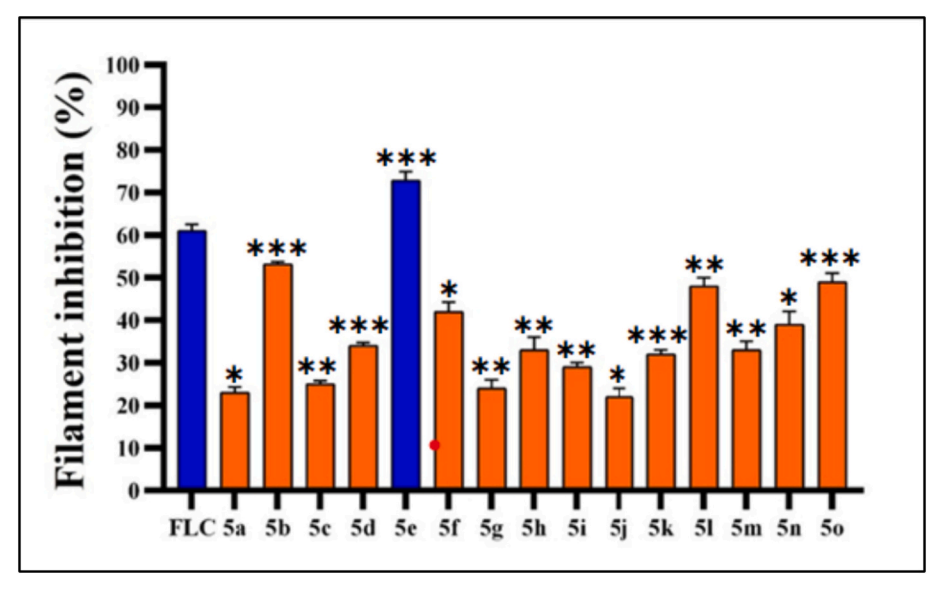
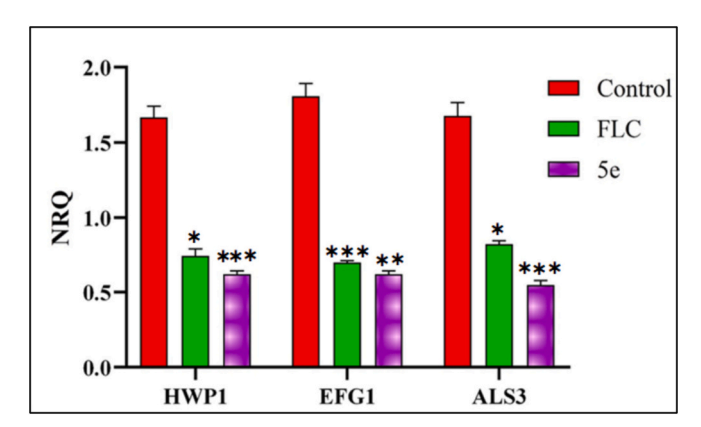


Fig. 9. Filament inhibition (%) of C. albicans by compounds 5(a-o) and FLC.



**Fig. 10.** Gene expression level of genes involved in the biofilm formation of *C. albicans* treated with 5e, FLC, and the control group (RPMI 1640 medium).

**Table 2** *C. albicans* biofilm gene expression using RT-PCR.

Gene	Control	FLC	5e
HWP1 EFG1	$1.7 \pm 0.1$ $1.8 \pm 0.1$	$0.75 \pm 0.05$ $0.7 \pm 0.05$	$0.6 \pm 0.05$ $0.6 \pm 0.05$
ALS3	$1.7 \pm 0.1$	$0.85 \pm 0.05$	$0.55 \pm 0.05$

These results establish the combined role of the ortho-OH group and long-chain substitution along with 1,3,4-oxadiazole nucleus, as a key structural motif for enhanced antifungal efficacy in this series (Fig. 13).42-44

#### 2.3. Molecular docking studies

Molecular docking studies were carried out to evaluate the binding affinity and interaction profile of compound **5e** with the standard antifungal agent fluconazole (FLC) against key virulence-associated proteins of *Candida albicans*, including ALS1, EFG1, and HWP1. Compound **5e** exhibited strong binding affinity towards the ALS1 protein, forming three hydrogen bonds with critical amino acid residues TYR21, LYS50, and ARG170, and achieved a docking score of -7.7, indicating a higher binding strength than the control FLC, which formed only two

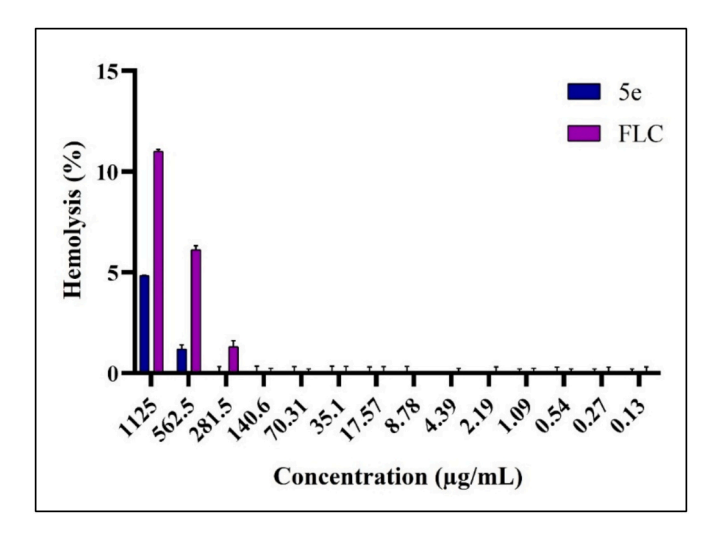


Fig. 11. Hemolytic activity of compound 5e and fluconazole (FLC). Compound 5e caused <8 % hemolysis at 1125  $\mu g/mL$ , while FLC showed 6.12 % and 11.0 % hemolysis at 562.5 and 1125  $\mu g/mL$ , respectively. No significant hemolysis was observed at lower concentrations. Data shown are mean  $\pm$  SD.

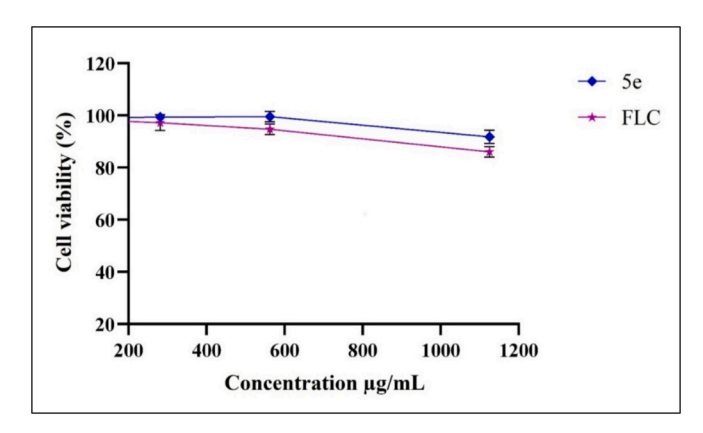


Fig. 12. The cytotoxic activity of compound 5e and fluconazole (FLC) in the concentration range of 200–1125  $\mu$ g/mL tested against mammalian cells. Results are expressed as percentage cell viability. Data shown are mean  $\pm$  SD.

Fig. 13. Representative functional properties of lead compound 5e.

hydrogen bonds with TYR21 and LYS59 and had a docking score of -4.4, which is likely to translate into more efficient inhibition of adhesion and biofilm formation. Similar trends have been reported in imidazole-derivative studies, where downregulation of ALS-family genes correlated with strong docking interactions to the ALS gene, supporting the biological relevance of such binding profiles.45 Against the transcriptional regulator EFG1 protein, compound **5e** formed three hydrogen bonds with SER226 and LYS240, resulting in a docking score of -3.4, while FLC formed two hydrogen bonds with MET447 and MET270, with a slightly better docking score of -4.0; this indicates functional interference in filamentation pathways. For the hyphal wall protein HWP1, compound 5e showed favourable interactions with three key residues CYS146, PRO347, and TYR395, yielding a docking score of -5.7, compared to FLC, which formed only one hydrogen bond with CYS346 and showed a docking score of -5.3; The enhanced bonding and binding energy with 5e suggest a stronger potential to block hyphal development. Prior docking studies targeting HWP1/Als-family proteins also highlighted that multiple H-bonds correlate with effective antibiofilm activity. Overall, multifaceted target engagement of 5e supports its candidacy as a next-generation antifungal agent that intervenes at multiple virulence checkpoints. Table 3 summarizes the docking results of the lead compound with three different targets, and Table 4 presents the overall docking outcome. Whereas Figs. 14, 15, and 16 represent the 2D interactions established with the lead molecule 5e and FLC with three different targets.

#### 2.4. In silico ADMET analysis

The pharmacokinetic behaviour and safety profiles of the fifteen synthesized compounds **5(a-o)** were evaluated using the ADMETlab 3.0 (https://admetlab3.scbdd.com).46 Key descriptors, including molecular weight, lipophilicity, topological polar surface area (TPSA), hydrogenbonding capacity, rotatable bond count, and synthetic accessibility (SA) scores, were analysed to assess their drug-like behaviour. All compounds possessed molecular weights below 500 Da, consistent with Lipinski's rule of five, indicating favourable oral drug-likeness. TPSA values for most compounds were below 90 Å<sup>2</sup>, suggesting good membrane permeability, except 50 (96 Å<sup>2</sup>), which slightly exceeded the optimal threshold. Rotatable bond counts were  $\leq 5$  across the series, reflecting an appropriate balance of flexibility and rigidity. Hydrogenbond donor (HBD) values were  $\leq 2$  for all derivatives, while hydrogen-bond acceptor (HBA) counts were less than or equal to 5 except for compound 5d, which exceeded the threshold. All the compounds that lack BBB permeability may offer peripheral selectivity with reduced CNS side effects.46 PAINS (Pan-Assay Interference Compounds) screening revealed zero alerts for all derivatives, ruling out structural

**Table 3** Hydrogen bonding interactions of 5e with key virulence proteins of *C. albicans*.

Target	Docking Score	H-bonding interactions
ALS1	−7.7	TYR21, LYS50, and ARG170
EFG1	−3.4	SER226 and LYS240
HWP1	−5.7	CYS146, PRO347, and TYR395

liabilities associated with non-specific biological activity. Synthetic accessibility (SA) scores ranged between 2.0 and 3.0, denoting easy-to-moderate feasibility of synthesis, thereby supporting the potential for analog expansion. Compounds 5(a-o), particularly 5e, exhibited a well-balanced ADME/Tox profile, fulfilling essential pharmacokinetic and drug-likeness parameters. These findings indicate that the *N-(5-undecyl-1,3,4-oxadiazol-2-yl)benzamide* is fundamentally sound; however, structural modifications aimed at improving solubility and metabolic compatibility would further strengthen its drug development potential. The results are depicted in the Table. 5. (See Table 6.)

#### 3. Conclusions

In summary, a novel series of N-(5-undecyl-1,3,4-oxadiazol-2-yl) benzamide derivatives was successfully synthesized and evaluated for antifungal and antibiofilm activities against Candida albicans. Among the tested compounds, compound 5e emerged as a promising lead, exhibiting superior activity in terms of MIC, MFC, with significant inhibition of biofilm and hyphal formation when compared to the standard antifungal drug fluconazole. The enhanced activity of compound 5e is attributed to the synergistic effect of its structural features, including the ortho-hydroxy benzamide group, the 1,3,4-oxadiazole core, and the long hydrophobic alkyl chain. Furthermore, RT-PCR analysis confirmed that compound 5e effectively downregulated key virulence genes (ALS1, ALS3, HWP1), while SEM imaging visually validated its antibiofilm efficacy. Hemolytic and cytotoxicity evaluations on human HEK293 cell line of lead compound 5e revealed negligible toxicity even at higher concentrations, highlighting the safety and suitability for further development. In addition, in silico molecular docking and ADMET studies further supported its favourable binding interactions and drug-like properties. Future studies should include proteomic profiling and target-based binding assays to validate whether the observed gene downregulation translates to protein-level effects and direct molecular interactions. Although our study was restricted to C. albicans, the downregulation of conserved biofilm-associated genes (e.g., ALS1, HWP1) indicates a possible broader relevance against nonalbicans Candida spp. Such approaches will provide deeper mechanistic insight into the antifungal action of compound 5e. These findings strongly suggest that compound 5e is a potential candidate for the development of a novel antifungal agent targeting biofilm-associated infections caused by Candida albicans.

#### 4. Experimental details

#### 4.1. Materials and methods

All chemicals and solvents were acquired from E. Merck (India), TCI Chemicals Ltd. and are used without further purification. Thin Layer Chromatography (TLC) analysis was done by utilizing Merck silica gel 60 F254 aluminium plates. The Stuart Digital Melting Point Apparatus (SMP 30) was used in determining the melting points of the compounds, which are uncorrected.  $^1\mathrm{H}$  and  $^{13}\mathrm{C}$  NMR spectra were recorded using Bruker (400 MHz for  $^1\mathrm{H}$  and 100 MHz for  $^{13}\mathrm{C}$ ) spectrometer using DMSO- $d_6$  as a solvent and tetramethylsilane (TMS) as the internal

**Table 4**Molecular docking results of compounds 5(a-o) with *C. albicans* biofilm-related genes.

Compound	Hyphal wall protein 1			Enhanced filamentous growth protein			Agglutinin-like growth sequence		
	Docking score	No. of H-bonds	Glide score	Docking score	No. of H-bonds	Glide score	Docking score	No. of H-bonds	Glide score
5a	-4.448	2	-4.787	-2.508	2	-2.874	-5.126	2	-5.466
5b	-5.186	2	-5.877	-2.214	3	-2.520	-3.665	3	-4.356
5c	-4.969	2	-5.191	-1.724	2	-1.946	-3.592	1	-3.814
5d	-7.149	3	-7.265	-2.431	2	-3.454	-3.252	1	-3.368
5e	-5.013	3	-5.703	-3.424	3	-4.114	-7.449	3	-6.870
5f	-4.628	2	-5.031	-3.062	2	-3.464	-4.400	2	-4.819
5g	-4.515	1	-4.518	-2.729	2	-2.732	_	_	_
5h	-3.373	1	-4.218	-3.394	1	-3.557	-4.055	2	-4.218
5i	-4.233	2	-4.473	-4.744	2	-5.395	-2.887	2	-3.539
5j	-3.793	2	-4.983	-2.749	1	-2.834	-4.658	2	-5.847
5k	-2.626	2	-2.890	-1.806	2	-2.070	-2.887	2	-3.539
51	-3.398	2	-3.405	-2.781	2	-2.789	-4.797	2	-4.805
5m	-3.507	2	-4.859	-1.036	2	-2.389	-4.559	2	-4.623
5n	-3.443	2	-3.934	-3.177	2	-3.517	-3.431	1	-3.771
5o	-5.879	1	-6.811	-3.667	2	-3.807	-3.993	2	-4.925
fluconazole	-5.359	1	-5.359	-4.056	2	-4.056	-4.494	2	-4.494

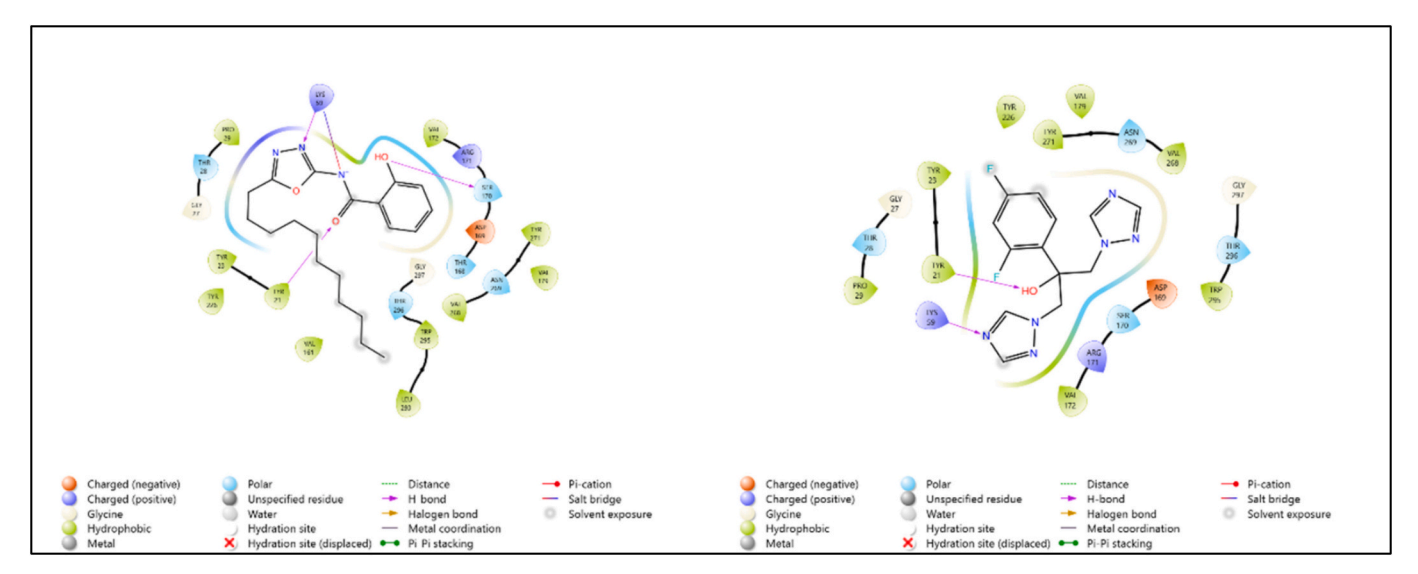


Fig. 14. 2D images of A) compound 5e molecular interaction with the amino acids of ALS1 B) FLC molecular interaction with the amino acids of ALS1.

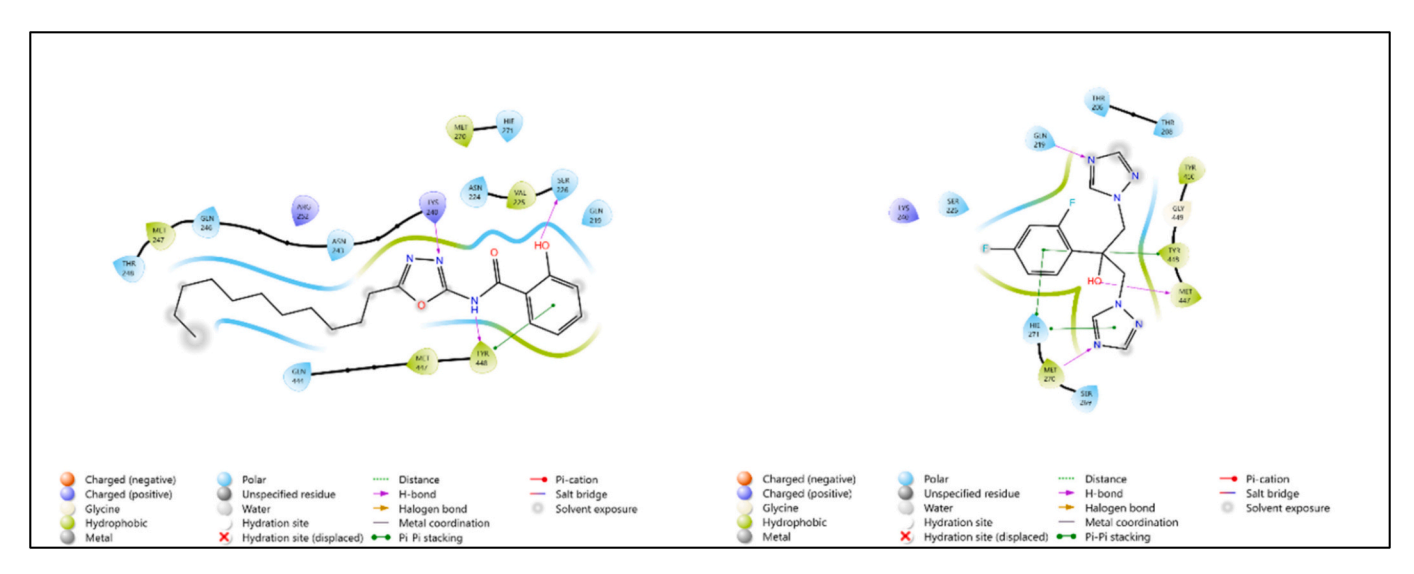


Fig. 15. 2D images of A) compound 5e molecular interaction with the amino acids of EFG1 B) FLC molecular interaction with the amino acids of EFG1.

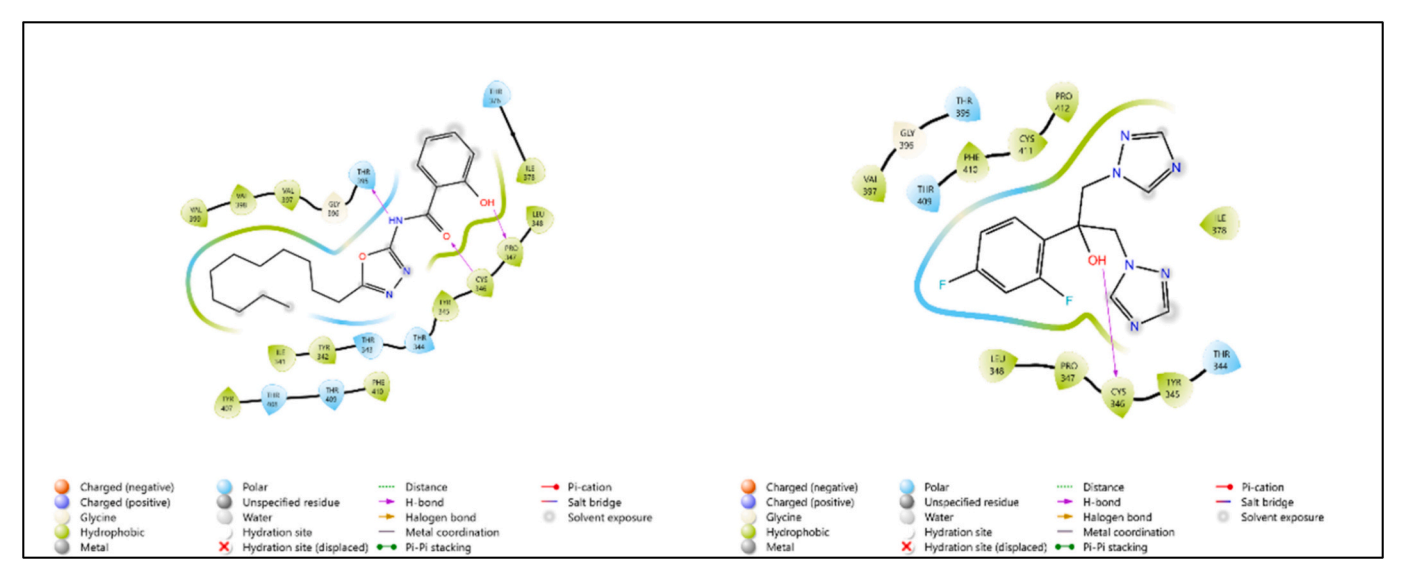


Fig. 16. 2D images of A) compound 5e molecular interaction with the amino acids of HWP 1 B) FLC molecular interaction with the amino acids of HWP1.

**Table 5**In silico ADME analysis of synthesized compounds 5(a-o).

Sl. No	Entry	Mw.	TPSA	HBA	HBD	LogP	SA	BBB Penetration	Lipinski's Violation	PAINS (in alerts)
1	5a	343.46	68.02	4	1	4.21	Easy	No	No	0
2	5b	344.45	80.91	5	1	3.54	Easy	No	No	0
3	5c	357.49	68.02	4	1	4.43	Easy	No	No	0
4	5d	373.49	77.25	5	1	4.37	Easy	No	No	0
5	5e	359.46	88.25	5	2	3.53	Easy	No	No	0
6	5f	361.45	68.02	5	1	4.13	Easy	No	No	0
7	5 g	433.42	68.02	9	1	3.98	Easy	No	No	0
8	5 h	377.91	68.02	4	1	4.23	Easy	No	No	0
9	5i	377.91	68.02	4	1	4.33	Easy	No	No	0
10	5j	422.36	68.02	4	1	4.16	Easy	No	No	0
11	5 k	422.36	68.02	4	1	4.48	Easy	No	No	0
12	51	378.9	80.91	5	1	3.71	Easy	No	No	0
13	5 m	423.35	80.91	5	1	3.89	Easy	No	No	0
14	5n	393.52	68.02	4	1	4.54	Easy	No	No	0
15	5o	349.49	96.26	4	1	4.31	Easy	No	No	0

**Table 6**Primers used in qPCR for *C. albicans* biofilm genes.

Target gene	GenBank accession No.	Sequence (5' to 3')	Product size (bp)	Temp (°C)	Ref.
ACT1	XM_019475182.1	F: TGGTGTTACTCACGTTGTTCA	184	57.9	51
		R: GGACAAATGGTTGGTCAAGCTC	174	57.2	
ALS3	XM_705343.2	F: ATTCGATCCTAACCGCGACA	179	58.1	
		R: TTGGTGCAGTTTTGGTCAGGT	180	57.3	
HWP1	P46593	F: CAGCCACTGAAACACCAACT	201	59.3	52
		R: CAGAAGTAACAACAACAACACCAG	194	58.9	
EFG1	XM_709144.2	F: GCACCAATCACCCCAAGTTC	164	56.2	51
	_	R: TTTGGCAACAGTGCTAGCTG	172	57.5	

standard. The chemical shifts were measured in  $\delta$  ppm downfield from tetramethylsilane. Mass analysis was determined by an Agilent QTOF mass spectrometer and was performed using ESI techniques.

# 4.2. General procedure for the synthesis of 5-undecyl-1,3,4-oxadiazol-2-amine (3)

A 100 mL dry round-bottom flask equipped with a magnetic stir bar was charged with lauric acid (1 mmol), semicarbazide hydrochloride (1 mmol), and phosphorus oxychloride (10 mL). The reaction mixture was stirred at 80  $^{\circ}\text{C}$  for 8–12 h. The progress of the reaction was monitored by thin-layer chromatography (TLC). After completion, the reaction mixture was cooled to 0  $^{\circ}\text{C}$  and carefully quenched by dropwise addition

of aqueous ammonia until the pH reached 7. Upon neutralization, a solid precipitate formed was collected by filtration and washed with cold water. The crude product was recrystallized from methanol to afford 5-undecyl-1,3,4-oxadiazol-2-amine (3) as a pure solid in good yield (98 %).

# 4.3. General procedure for the synthesis of N-(5-undecyl-1,3,4-oxadiazol-2-yl)benzamide derivatives **5(a-o)**

To a stirred solution of substituted aromatic acids **4(a–o)** (1.0 mmol) in dry THF at 0  $^{\circ}$ C (ice bath), 1-hydroxybenzotriazole (HOBt) (1.5 mmol) and triethylamine (2.0 mmol) were added. The reaction mixture was stirred for 10 min, after which EDCI (2.0 mmol) was added. Stirring

was continued for an additional 15 min, followed by the addition of 5-undecyl-1,3,4-oxadiazol-2-amine (1.0 mmol). The reaction was further stirred at room temperature for 2–3 h. Completion of the reaction was monitored by TLC. After completion of the reaction, the mixture was extracted with ethyl acetate and water (3× 30 mL). The combined organic layers were separated and dried over anhydrous Na<sub>2</sub>SO<sub>4</sub>, and concentrated under reduced pressure. The crude product was purified by silica gel column chromatography to get the desired compounds 5(a-o).

#### 4.3.1. N-(5-undecyl-1,3,4-oxadiazol-2-yl)benzamide (5a)

Appearance: Colourless solid (Amorphous); m. $p=114-116\,^{\circ}$ C;  $^{1}$ H NMR (400 MHz, CDCl<sub>3</sub>)  $\delta$  7.96 (dd, 2H, J=4 Hz, 8 Hz), 7.55 (dd, 1H, J=4 Hz, 8 Hz), 7.49–7.45 (m, 2H), 5.63 (s, 1H), 2.86 (t, 2H, J=8 Hz), 1.93–1.87 (m, 2H), 1.39–1.25 (m, 16H), 0.90–0.87 (m, 3H);  $^{13}$ C NMR (101 MHz, CDCl<sub>3</sub>)  $\delta$  165.30, 161.02, 158.36, 133.10, 131.90, 128.61, 128.29, 31.87, 29.65, 29.64, 29.43, 29.41, 29.34, 28.63, 27.12, 24.86, 22.72, 14.08. LC-MS (ESI, m/z) calcd. For C<sub>20</sub>H<sub>29</sub>N<sub>3</sub>O<sub>2</sub> 343.4710; found (M + H)<sup>+</sup> 344.4608.

#### 4.3.2. N-(5-undecyl-1,3,4-oxadiazol-2-yl)picolinamide (5b)

Appearance: Colourless solid (Amorphous); m.p=116-118 °C;  $^1\mathrm{H}$  NMR (400 MHz, CDCl<sub>3</sub>)  $\delta$  8.60 (d, 1H, J=8 Hz), 8.21 (d, 1H, J=4 Hz), 7.90–7.86 (m, 1H), 7.49–7.47 (m, 1H), 5.34 (s, 1H), 2.69 (t, 2H, J=4 Hz, 8 Hz), 1.71–1.69 (m, 2H), 1.40–1.27 (m, 16H), 0.89 (t, 2H, J=4 Hz);  $^{13}\mathrm{C}$  NMR(101, MHz, CDCl<sub>3</sub>)  $\delta$  167.17, 163.01, 161.99, 149.54, 148.34, 137.32, 126.50, 122.45, 122.34, 31.90, 29.71, 29.59, 29.43, 29.32, 29.15, 28.96, 26.37, 25.93, 25.35, 22.69, 14.12. LC-MS (ESI, m/z) calcd. For C<sub>19</sub>H<sub>28</sub>N<sub>4</sub>O<sub>2</sub> 344.2212; found (M + H)<sup>+</sup> 345.6618.

#### 4.3.3. 4-methyl-N-(5-undecyl-1,3,4-oxadiazol-2-yl)benzamide (5c)

Appearance: Colourless solid (Amorphous); m, $p=110-112\,^{\circ}\mathrm{C}$ ;  $^{1}\mathrm{H}$  NMR (400 MHz, CDCl<sub>3</sub>)  $\delta$  7.73 (d, 2H, J=8 Hz), 7.26 (dd, 2H, J=8 Hz, 12 Hz), 6.31 (s, 1H), 2.68 (t, 2H, J=4 Hz, 8 Hz), 2.42 (s, 3H), 1.76–1.68 (m, 2H), 1.38–1.24 (m, 16H) 0.89 (t, 3H, J=4 Hz);  $^{13}\mathrm{C}$  NMR (101 MHz, CDCl<sub>3</sub>)  $\delta$  169.75, 163.16, 161.45, 142.52, 130.53, 129.28, 127.40, 31.91, 29.71, 29.60, 29.48, 29.43, 29.33, 29.16, 28.97, 26.36, 25.34, 22.69, 21.49, 14.13. LC-MS (ESI, m/z) calcd. For C<sub>21</sub>H<sub>31</sub>N<sub>3</sub>O<sub>2</sub> 357.2416; found (M + H)<sup>+</sup> 358.0815.

#### 4.3.4. 4-methoxy-N-(5-undecyl-1,3,4-oxadiazol-2-yl)benzamide (5d)

Appearance: Colourless solid (Amorphous); m.p=112-114 °C;  $^1\mathrm{H}$  NMR (400 MHz, CDCl<sub>3</sub>)  $\delta$  7.80 (dd, 2H, J=4 Hz, 8 Hz), 6.95 (dd, 2H, J=4 Hz, 8 Hz), 5.95 (s, 1H, Br), 3.88 (s, 3H), 2.70 (t, 2H, J=8 Hz), 1.81–1.70 (m, 9H), 1.41–1.28 (m, 9H), 0.92–0.88 (m, 3H);  $^{13}\mathrm{C}$  NMR (101 MHz, CDCl<sub>3</sub>)  $\delta$  173.99, 172.96, 168.97, 162, 61, 129.30, 125.57, 113.81, 55.45, 31.91, 29.59, 29.33, 29.15, 28.97, 26.38, 25.35, 22.69, 14.13. LC-MS (ESI, m/z) calcd. For C<sub>21</sub>H<sub>31</sub>N<sub>3</sub>O<sub>3</sub> 373.2365; found (M + H)<sup>+</sup> 374.3070.

#### 4.3.5. 2-hydroxy-N-(5-undecyl-1,3,4-oxadiazol-2-yl)benzamide (5e)

Appearance: Off white solid (Amorphous); m.p=114-116 °C;  $^1\mathrm{H}$  NMR (400 MHz, CDCl<sub>3</sub>)  $\delta$  8.77 (s, 1H), 6.51–6.09 (m, 4H), 4.99 (s, 1H), 2.71 (t, 2H, J=8 Hz), 1.77–1.62 (m, 6H), 1.43–1.19 (m, 12H), 0.90 (t, 3H, J=8 Hz);  $^{13}\mathrm{C}$  NMR (101 MHz, CDCl<sub>3</sub>)  $\delta$  170.66, 162.93, 161.73, 159.29, 145.91, 141.70, 139.06, 136.34, 124.70, 31.90, 29.58, 29.41, 29.31, 29.13, 28.95, 26.35, 25.33, 22.67, 14.09; LC-MS (ESI, m/z) calcd. For  $\mathrm{C}_{20}\mathrm{H}_{29}\mathrm{N}_{3}\mathrm{O}_{3}$  359.2209; found (M + H) $^{+}$  360.5124.

#### 4.3.6. 4-fluoro-N-(5-undecyl-1,3,4-oxadiazol-2-yl)benzamide (5f)

Appearance: Colourless solid (Amorphous); m.p=126-128 °C;  $^{1}\mathrm{H}$  NMR (400 MHz, CDCl<sub>3</sub>)  $\delta$  8.10 (s, 2H), 7.38 (dd, 2H, J=7.2 Hz, 15.2 Hz), 6.58(s, 1H), 2.94 (m, 3H), 1.97 (m, 3H), 1.52 (m, 16H), 1.14(s, 3H);  $^{13}\mathrm{C}$  NMR(101 MHz, CDCl<sub>3</sub>)  $\delta$  165.18, 164.83, 162.81, 160.88, 158.29, 130.31, 130.25, 130.01, 129.99, 115.86, 115.70, 31.87, 29.64, 29.64, 29.43, 29.01, 28.62, 26.76, 24.95, 22.72, 14.09; LC-MS (ESI, m/z) calcd. For C<sub>20</sub>H<sub>28</sub>FN<sub>3</sub>O<sub>2</sub> 361.2166; found (M + H)<sup>+</sup> 362.1557.

# 4.3.7. 2,3,4,5,6-pentafluoro-N-(5-undecyl-1,3,4-oxadiazol-2-yl) benzamide (5 g)

Appearance: Colourless solid (Amorphous); m.p=151-153 °C;  $^{1}\mathrm{H}$  NMR (400 MHz, CdCl<sub>3</sub>)  $\delta$  5.24 (s, 1H), 2.70 (t, 2H, J=8 Hz, 12 Hz), 1.73 (t, 2H, J=8 Hz), 1.39–1.28 (m, 16H), 0.89 (t, 3H, J=4 Hz, 8 Hz);  $^{13}\mathrm{C}$  NMR (101 MHz, CDCl<sub>3</sub>)  $\delta$  171.23, 162.94, 161.52, 159.01, 147.72, 133.65, 124.70, 31.90, 29.59, 29.42, 29.33, 29.15, 28.96, 26.36, 25.34, 22.69, 14.12; LC-MS (ESI, m/z) calcd. For C<sub>20</sub>H<sub>24</sub>F<sub>5</sub>N<sub>3</sub>O<sub>2</sub> 433.4230; found (M + H) 434.5201.

#### 4.3.8. 3-chloro-N-(5-undecyl-1,3,4-oxadiazol-2-yl)benzamide (5h)

Appearance: Colourless solid (Amorphous); m,p=132-134 °C;  $^1\mathrm{H}$  NMR (400 MHz, CdCl<sub>3</sub>)  $\delta$  7.84 (s, 1H), 7.71 (d, 1H, J=8 Hz), 7.51 (d, 1H, J=8 Hz), 7.41 (dd, 1H, J=4 Hz, 8 Hz), 5.28 (s, 1H), 2.70 (t, 2H, J=8 Hz), 1.75–1.71 (m, 2H), 1.39–1.28 (m, 16H), 0.90 (t, 3H, J=8 Hz);  $^{13}\mathrm{C}$  NMR (101 MHz, CDCl<sub>3</sub>)  $\delta$  168.25, 163.03, 161.47, 135.18, 134.84, 132.04, 129.96, 127.76, 125.42, 31.91, 29.60, 29.43, 29.33, 29.16, 28.97, 26.37, 25.35, 22.69, 14.13. LC-MS (ESI, m/z) calcd. For  $\mathrm{C}_{20}\mathrm{H}_{28}\mathrm{ClN}_{3}\mathrm{O}_{2}$  377.1870; found (M + H)<sup>+</sup> 377.9782.

#### 4.3.9. 4-chloro-N-(5-undecyl-1,3,4-oxadiazol-2-yl)benzamide (5i)

Appearance: Colourless solid (Amorphous); m. $p=138-140\,^{\circ}\text{C}$ ;  $^{1}\text{H}$  NMR (400 MHz, CDCl<sub>3</sub>)  $\delta$  7.85 (dd, 2H,  $J=4\,\text{Hz}$ , 8 Hz), 7.15 (dd, 2H,  $J=8\,\text{Hz}$ ,16 Hz), 5.92 (s, 1H), 2.71 (t, 2H,  $J=8\,\text{Hz}$ ), 1.78–1.20 (m, 18H), 0.92–0.88 (m, 3H);  $^{13}\text{C}$  NMR(101 MHz, CDCl<sub>3</sub>)  $\delta$  168.51, 138.47, 131.72, 131.44, 129.01, 128.88, 77.42, 77.10, 76.78, 31.97, 29.66, 29.49, 29.40, 29.22, 29.03, 26.42, 25.40, 22.76, 14.20. LC-MS (ESI, m/z) calcd. For  $\text{C}_{20}\text{H}_{28}\text{ClN}_{3}\text{O}_{2}$  377.1870; found (M + H) $^{+}$  378.9657.

#### 4.3.10. 2-bromo-N-(5-undecyl-1,3,4-oxadiazol-2-yl)benzamide (5j)

Appearance: Colourless solid (Amorphous); m. $p=140-142\,^{\circ}\mathrm{C}$ ;  $^{1}\mathrm{H}$  NMR (400 MHz, CDCl<sub>3</sub>)  $\delta$  7.40 (dd, 1H, J=4 Hz, 8 Hz), 7.32 (dd, 1H, J=4 Hz, 8 Hz), 6.46 (s, 1H), 6.20 (s, 1H), 5.21 (s, 1H), 2.69 (t, 2H, J=8 Hz), 2.31 (m, 2H), 1.76–1.66 (m, 4H), 1.42–1.18 (m, 12H), 0.85 (t, 3H, J=8 Hz);  $^{13}\mathrm{C}$  NMR(101 MHz, CDCl<sub>3</sub>)  $\delta$  169.51, 136.74, 133.67, 131.76, 129.96, 127.70, 127.68, 119.28, 31.97, 29.66, 29.50, 29.40, 29.22, 29.03, 26.43, 25.41, 22.76, 14.20; LC-MS (ESI, m/z) calcd. For  $\mathrm{C}_{20}\mathrm{H}_{28}\mathrm{BrN}_{3}\mathrm{O}_{2}$  422.3670; found (M + H)<sup>+</sup> 423.2718.

#### 4.3.11. 4-bromo-N-(5-undecyl-1,3,4-oxadiazol-2-yl)benzamide (5 k)

Appearance: Colourless solid (Amorphous); m.p=158-160 °C;  $^{1}\mathrm{H}$  NMR (400 MHz, CDCl<sub>3</sub>)  $\delta$  7.71 (dd, 2H, J=4 Hz, 8 Hz), 7.62 (dd, 2H, J=8 Hz, 4 Hz), 6.07 (s, 1H), 2.28 (t, 2H, J=8 Hz), 1.74–1.64 (m, 8H), 1.30–1.27 (m, 10H), 0.92–0.86 (m, 3H);  $^{13}\mathrm{C}$  NMR (101 MHz, CDCl<sub>3</sub>)  $\delta$  168.51, 138.47, 133.6, 131.72, 131.44, 129.01, 128.88, 31.97, 29.66, 29.49, 29.40, 29.22, 29.03, 26.42, 25.40, 22.76, 14.20; LC-MS (ESI, m/z) calcd. For  $\mathrm{C}_{20}\mathrm{H}_{28}\mathrm{BrN}_{3}\mathrm{O}_{2}$  422.3670; found (M + H) $^{+}$  423.1870.

#### 4.3.12. 2-chloro-N-(5-undecyl-1,3,4-oxadiazol-2-yl)nicotinamide (5 l)

Appearance: Colourless solid (Amorphous); m. $p=165-167\,^{\circ}\mathrm{C}$ ;  $^{1}\mathrm{H}$  NMR (400 MHz, CDCl<sub>3</sub>)  $\delta$  8.51 (d, 1H, J=8 Hz), 8.21 (d, 1H, J=8 Hz), 7.38 (dd, 1H, J=4 Hz, 12 Hz), 5.40 (s, 1H), 2.67 (t, 2H, J=8 Hz), 1.72–1.27 (m, 18H), 0.89 (t, 3H, J=8 Hz);  $^{13}\mathrm{C}$  NMR (101 MHz, CDCl<sub>3</sub>)  $\delta$ 166.39, 163.13, 163.07, 161.38, 151.42, 150.16, 140.29, 122.85, 31.90, 29.59, 29.43, 29.33, 29.15, 28.91, 26.35, 25.33, 22.69, 14.12; LC-MS (ESI, m/z) calcd. For C<sub>19</sub>H<sub>27</sub>ClN<sub>4</sub>O<sub>2</sub> 378.9010; found (M + H)<sup>+</sup> 380.3792.

### 4.3.13. 2-bromo-N-(5-undecyl-1,3,4-oxadiazol-2-yl)isonicotinamide (5 m)

Appearance: Colourless solid (Amorphous); m.p=162–164 °C;  $^1\mathrm{H}$  NMR (400 MHz, CDCl<sub>3</sub>)  $\delta$  8.50 (d, 1H, J=4 Hz), 7.97 (s, 1H), 7.77(d, 1H, J=4 Hz), 6.82(s, 1H), 2.59 (t, 2H, J=4 Hz, 8 Hz), 1.56 (t, 2H, J=4 Hz, 8 Hz), 1.29–1.12(m, 16H), 0.82 (t, 3H, J=4 Hz, 8 Hz);  $^{13}\mathrm{C}$  NMR (101 MHz, CDCl<sub>3</sub>)  $\delta$  165.55, 163.94, 160.05, 151.66, 144.84, 142.30, 126.23, 121.73, 31.69, 29.37, 29.26, 29.09, 28.94, 28.65, 26.29, 24.87,

22.51, 14.38. LC-MS (ESI, m/z) calcd. For  $C_{19}H_{27}BrN_4O_2$  423.3550; found  $(M + H)^+$  424.4030.

#### 4.3.14. N-(5-undecyl-1,3,4-oxadiazol-2-yl)-2-naphthamide (5n)

Appearance: Light brown solid (Amorphous); m. $p=108-110\,^{\circ}$ C;  $^{1}$ H NMR (400 MHz, CDCl<sub>3</sub>)  $\delta$  9.12 (d, 1H, J=8 Hz), 8.44 (dd, 1H, J=8 Hz), 8.12 (d, 1H, J=12 Hz), 7.95 (d, 1H, J=8 Hz), 7.64 (m, 1H), 7.57 (d, 2H, J=8 Hz), 4.25 (s, 1H), 2.42 (dd, 1H, J=4 Hz,8 Hz), 1.45–1.24 (m, 17H), 0.97–0.86 (m, 6H);  $^{13}$ C NMR (101 MHz, CDCl<sub>3</sub>)  $\delta$  172.80, 134.59, 133.95, 131.81, 130.92, 128.73, 128.10, 126.44, 125.94, 125.69, 124.57, 68.20, 38.74, 30.38, 29.73, 29.61, 28.94, 23.76, 23.0, 14.14, 14.07, 10.98; LC-MS (ESI, m/z) calcd. For C<sub>24</sub>H<sub>31</sub>N<sub>3</sub>O<sub>2</sub> 393.5310; found (M + H)<sup>+</sup> 394.9521.

4.3.15. N-(5-undecyl-1,3,4-oxadiazol-2-yl)thiophene-2-carboxamide (5o) Appearance: Colourless solid (Amorphous); m.p = 128–130 °C;  $^1\mathrm{H}$  NMR (400 MHz, CDCl<sub>3</sub>)  $\delta$  7.55 (dd, 2H, J = 4 Hz, 8 Hz), 7.12 (dd, 1H, J = 4 Hz, 8 Hz), 5.13 (s, 1H), 2.70 (t, 3H, J = 4 Hz, 8 Hz), 1.77–1.67 (m, 2H), 1.39–1.28 (m, 16H), 0.90 (t, 3H, J = 8 Hz);  $^{13}\mathrm{C}$  NMR (101 MHz, CDCl<sub>3</sub>)  $\delta$  172.89, 162.89, 161.52, 137.85, 130.94, 129.28, 127.81, 31.91, 29.60, 29.43, 29.33, 29.16, 28.97, 26.37, 25.35, 22.69, 14.13; LC-MS (ESI, m/z) calcd. For  $\mathrm{C_{18}H_{27}N_{3}O_{2}S}$  349.4930; found (M + H)<sup>+</sup> 350.0193.

#### 5. Biological evaluations

#### 5.1. Candida species and culture conditions

Candida albicans MTCC 198 was procured from the Microbial Type Culture Collection (MTCC), Chandigarh, India. The strain was initially revived on Sabouraud Dextrose Agar (SDA; HiMedia Laboratories, India) and incubated at 37 °C for 48 h. A single well-isolated colony was then inoculated into Sabouraud Dextrose Broth (SDB; HiMedia) and incubated at 37 °C for 18–24 h to obtain actively growing yeast cells for experimental use. Cell density was adjusted to an optical density of 0.2 at 600 nm (equivalent to approximately  $1\times 10^6$  CFU/mL) before further assays. All procedures were performed under aseptic conditions to prevent contamination.

## 5.2. Evaluation of antifungal activities by broth microdilution (BMD) method

The minimum inhibitory concentrations (MICs) and minimum fungicidal concentrations (MFCs) of the synthesized compounds 5(a-o) and the reference drug fluconazole (FLC) against Candida albicans were determined using the broth microdilution (BMD) method, following the Clinical and Laboratory Standards Institute (CLSI) M27-S4 guidelines, 47 as previously described by Salari and Ghasemi Nejad Almani (2020).48 The BMD assay was carried out in sterile 96-well microtiter plates using RPMI 1640 medium (Sigma-Aldrich, USA) buffered with MOPS (Sigma-Aldrich, USA). Fluconazole and test compounds were initially dissolved in dimethyl sulfoxide (DMSO; Sigma-Aldrich, USA), followed by dilution in RPMI 1640 medium to prepare two-fold serial dilutions ranging from 1125 to 0.125 µg/mL. A standardized inoculum of C. albicans  $(1.5 \times 10^3)$ CFU/mL) in RPMI 1640 medium was added to each well containing the drug dilutions. The plates were incubated at 35 °C for 24 h in a shaking incubator at 100 rpm. MIC values were determined spectrophotometrically at 570 nm using a microplate reader and defined as the lowest concentration of the compound that resulted in ≥50 % inhibition of fungal growth compared to the untreated control wells. All experiments were performed in triplicate, and average MIC values are reported in  $\mu g$ mL. To determine the MFC values, 10  $\mu$ L aliquots from wells showing no visible growth were subcultured onto Sabouraud Dextrose Agar (SDA) plates and incubated at 35 °C for 24 h. MFC was defined as the lowest drug concentration that yielded three or fewer colonies, indicating ≥99.9 % fungicidal activity against the initial inoculum.

#### 5.3. Biofilm inhibition activity

The Biofilm inhibition activity of compounds 5(a-o) and fluconazole (FCL) against C. albicans was evaluated by the crystal violet quantification method in 96-well microtiter plates according to the protocol reported by Aati et al., with slight modifications.49 Briefly, 150 μL of a 10 CFU/mL suspension of C. albicans was added to the wells of a sterile 96-well microtiter plate (Greiner, Germany), followed by the addition of 100 µL of each compound and FLC at their respective MIC concentrations prepared in RPMI 1640 medium (Sigma Aldrich, USA) buffered with 0.165 M MOPS (Sigma Aldrich. USA). Wells containing only C. albicans without any compounds served as the untreated control. After 24 h of incubation at 35 °C in a shaking incubator at 100 rpm, the non-adherent cells were gently removed, and the wells were washed twice with sterile PBS (pH 7.0). Subsequently, 100 µL of 99 % methanol was added to each well and left for 15 min for fixation. The methanol was removed, and the plates were air-dried. Then, 100  $\mu L$  of 0.1 % crystal violet solution was added to each well and incubated for 10-15 min. The excess stain was discarded, and the wells were gently rinsed with tap water and air-dried. Finally, the absorbance was measured at 590 nm using a microplate reader (BioTek Co., USA) to quantify the biofilm biomass. All experiments were conducted in triplicate, and the mean absorbance values along with standard deviations were calculated to assess reproducibility and variability between replicates. The percentage reduction in the biofilm formation of Candida sp. was calculated

Percent of Inhibition = 
$$\left(1 - \frac{ODA}{ODB}\right) \times 100$$

where ODA = Absorbance of well containing CFNS+Candida sp. ODB = Absorbance of well containing Candida sp. (Control).

#### 5.4. Filament inhibition assay

The Filament inhibition activity of compounds 5(a-o) and FLC against C. albicans was assessed by a filament inhibition assay according to the methodology described by Wang et al., with slight modifications. 50 Briefly, in a sterile 2 mL Eppendorf tube, 100 µL of C. albicans suspension at a concentration of  $1 \times 10^7$  CFU/mL was mixed with 300 μL of each compound 5(a-o) and FLC at their respective MIC concentrations, and the total volume was adjusted to 900 µL with RPMI 1640 medium (Sigma Aldrich, USA) buffered with 0.165 M MOPS (Sigma Aldrich, USA) and incubated statically at 37 °C for 4 h. The wells containing only Candida spp. were considered controls. After incubation, the suspensions were vortexed for 20 s, and 20 µL of each mixture was loaded into a Neubauer counting chamber (V3 Scientific Solutions, India). Filamented and non-filamented cells were counted manually, with 100 cells observed per field, and the percentage of filamented cells was calculated. The filamentation rates of C. albicans treated with each azole compound and FLC were compared to the untreated control group to determine the inhibitory effect. All assays were performed in triplicate, and the average results with standard deviations were calculated to ensure reproducibility.

#### 5.5. Analysis of C. albicans biofilm gene expression using RT-PCR

The inhibitory effects of the lead compound **5e** and fluconazole (FLC) on the transcription of biofilm-related genes in *C. albicans* were evaluated using quantitative real-time polymerase chain reaction (qRT-PCR) according to the methodology described by Rossoni et al. (2020) with slight modifications.51 Biofilms were formed on 6-well plates following the same protocol as used for the SEM sample preparation. After 24 h of biofilm development in the presence of compound **5e** at its MIC concentration, the total RNA was extracted using RNAiso Plus reagent (Cat. #9108/9109, Takara Biosciences, Japan) according to manufacturer

guidelines. The RNA concentration, purity, and quality were assessed using a NanoDrop 2000 spectrophotometer (Thermo Fisher Scientific Inc., Wilmington, DE, USA). One microgram of total RNA was reverse transcribed into complementary DNA (cDNA) using the PrimeScript<sup>TM</sup> RT reagent Kit (Takara Biosciences, Cat. #RR037A) according to the manufacturer's instructions, and cDNA samples were stored at  $-80~^{\circ}\text{C}$ until use. The specific primers (Table 1) for the biofilm genes ALS3, HWP1, EFG1, and reference gene ACT1 analysed in the present study were described and used as indicated by Rossoni et al. (2020). Quantitative PCR reactions were performed using TB Green Premix Ex Taq II (Tli RNaseH Plus) (Cat. #RR037A 202,202 Da, Takara Biosciences) in a Qiagen RT-PCR cycler. Each reaction included cDNA, gene-specific primers, and master mix, while no-template controls were set by adding all reagents except cDNA. The thermal cycling conditions were: initial denaturation at 95 °C for 30 s (Cycle 1, hold), followed by 40 cycles of denaturation at 95 °C for 5 s and annealing/extension at 60 °C for 30 s. Following amplification, a melting curve analysis was performed to verify specificity. Gene expression levels were normalized to the ACT1 reference gene, which was tested across all groups. The relative quantification of gene expression was calculated using the  $2^{-\Delta \Delta CT}$ method, and the expression levels in treated samples were compared with those of the control group treated with DMSO-diluted RPMI medium.53

#### 6. Erythrocyte hemolysis assay

The hemolytic potential of compound 5e was evaluated using a standardized erythrocyte lysis assay with sheep red blood cells, following protocols with minor modifications (Turecka et al., 2018). Fresh sheep blood was collected in anticoagulant-coated tubes and centrifuged at 1000  $\times g$  for 10 min to separate erythrocytes. The pellet was washed three times with sterile 0.9 % NaCl solution to remove plasma and leukocytes and resuspended to prepare a 2 % erythrocyte suspension. Aliquots of 100 µL of the erythrocyte suspension were dispensed into the wells of a 96-well microtiter plate and incubated at 37 °C with two-fold serial dilutions of compound 5e and fluconazole in the concentration range of 1125 to  $0.125 \mu g/mL$  (diluted in saline). As controls, 4 % Triton X-100 (representing 100 % lysis) and saline solution (0 % lysis) were included. Following incubation for 1 h at 37 °C, the plates were centrifuged at 1000 ×g for 10 min to pellet unlysed erythrocytes. The supernatants were carefully transferred to fresh plates, and the absorbance was recorded at 450 nm using a microplate reader.

Percentage hemolysis was calculated according to the formula:

$$\% Hemolysis = \frac{(A450 sample - A450 saline\ control)}{(A450 Triton\ control - A450 saline\ control)} \times 100$$

All experiments were conducted in triplicate, and results were expressed as mean  $\pm$  SD.

#### 6.1. Cytotoxicity assay on HEK293 cells

The human embryonic kidney cell line HEK293 was obtained from the NCCS Cell Repository (Pune, India). Cells were cultured in Minimum Essential Medium (MEM, Eagle) supplemented with 2 mM  $_{\rm L}$ -glutamine, non-essential amino acids (NEAA), 10 % heat-inactivated fetal bovine serum (FBS), and 1 % penicillin–streptomycin. All cultures were maintained in a humidified incubator at 37 °C with 5 % CO $_{\rm 2}$  and 95 % relative humidity. Subculturing was performed at  $\sim\!80$  % confluency, and cells were routinely monitored using an inverted phase-contrast microscope. The cytotoxicity of compound 5e and the reference antifungal fluconazole (FLC) was determined using the MTT assay, as described by Turecka et al. (2018)54 with minor modifications. Briefly, HEK293 cells were seeded in 96-well flat-bottom microplates at a density of 5  $\times$  10 $^3$  cells/well in 100  $\mu$ L of complete medium and incubated for 24 h. The cells were then treated with two-fold serial dilutions of compound 5e and fluconazole in the concentration range of 1125 to 0.125  $\mu$ g/mL

(prepared in saline) for 24 h. Plates were incubated at 37  $^{\circ} C$  for 4 h, after which the formazan crystals were dissolved in 100  $\mu L$  of DMSO. Absorbance was measured at 550 nm using a microplate spectrophotometer. The absorbance of untreated cells was considered 100 % viability, and results were expressed as the percentage of viable cells relative to the control. Each treatment was performed in triplicate, and data are presented as mean  $\pm$  SD.

#### 6.2. Scanning electron microscopy (SEM) analysis of biofilm inhibition

The antifungal activity of compound (5e) and FLC on the biofilm structure of C. albicans was evaluated by scanning electron microscopy (SEM) according to the methodology described by Barbosa et al. (2016) with minor modifications.55 Briefly, sterile glass coverslips measuring 8 mm in diameter were placed into the wells of a 6-well plate. Each well was added with 1.5 mL of RPMI 1640 medium (Sigma Aldrich, USA) buffered with 0.165 M MOPS (Sigma Aldrich, USA), followed by the addition of compound 5e and FLC at their respective MIC concentrations. Subsequently, 20  $\mu$ L of *C. albicans* suspension at  $1 \times 10^7$  CFU/mL was inoculated into each well and incubated at 37  $^{\circ}$ C for 24 h. The wells containing only Candida spp. were considered controls. After incubation, the coverslips containing biofilms were gently washed with phosphate-buffered saline (PBS, pH 7.0) and fixed with 1 mL of 2.5 % glutaraldehyde for 1 h at room temperature. The samples were then subjected to a graded ethanol dehydration series (10 %, 30 %, 50 %, 70 %, and 90 % ethanol) for 20 min at each concentration, followed by immersion in 100 % ethanol for 1 h. The specimens were subsequently air-dried by incubating at 37 °C for 24 h. After complete drying, the coverslips were mounted onto aluminium stubs, sputter-coated with gold, and observed under a scanning electron microscope (EVO LS 15, Carl Zeiss, Germany) at 4000× magnification at the Institute of Excellence, University of Mysuru, Mysuru, India.

#### 6.3. Molecular docking

The antibiofilm potential of selected compounds 5(a-o) was further evaluated through in silico molecular docking studies using the Schrödinger software suite-2021-24, Maestro 14.0 edition (Schrödinger LLC, NY, USA), according to the methodology described by Gundogdu et al. (2025).56 Structure-based docking targeted biofilm-associated proteins that were significantly downregulated in gene expression analysis, including Hyphal Wall Protein 1 (HWP1), Enhanced Filamentous Growth protein 1 (EFG1), and Agglutinin-Like Sequence 1 (ALS1). Due to the unavailability of these protein structures in the Protein Data Bank (PDB), their 3D structures were retrieved from the AlphaFold Protein Structure Database (https://alphafold.ebi.ac.uk, accessed on 27 April 2025). Ligands, including the test compounds and standard antifungal drug FLC, were drawn using a 2D sketcher and prepared using the LigPrep module of Schrodinger software to ensure correct ionization, stereochemistry, and tautomeric states. Protein targets were processed using the protein preparation wizard of Schrodinger software to assign bond orders, optimize hydrogen bonding, and add missing atoms. Docking was performed using the Glide XP (extra precision) module of Schrodinger software in flexible mode, with a grid size of 30 Å. After docking, the molecular interaction was visualized using the ligand interaction tool, emphasizing crucial hydrogen bonds and hydrophobic contacts with particular amino acids within the protein. The binding affinity of each ligand was evaluated based on the Docking Score (DScore).

#### 6.4. In silico ADMET analysis

In this study, the ADMET (Absorption, Distribution, Metabolism, Excretion, and Toxicity) profiling of the synthesized compounds 5(a-o) was carried out using ADMETlab 3.0 (https://admetmesh.scbdd.com/), an integrated platform for comprehensive pharmacokinetic and

toxicological evaluation. The molecular structures of the compounds were drawn using ChemSketch, and their corresponding SMILES (Simplified Molecular Input Line Entry Specification) notations were generated for input into the ADMETlab system. The predictive models analysed multiple pharmacokinetic and drug-likeness parameters, including blood-brain barrier (BBB) permeability, Lipinski's Rule of Five, with emphasis on molecular weight (100–600 Da), hydrogen bond acceptors (HbA), hydrogen bond donors (HbD), and topological polar surface area (TPSA 0–140 Å $^2$ ). Potential pan-assay interference compounds (PAINS) alerts were also evaluated. $^{57},^{58}$ 

#### 6.5. Statistical analysis

The GRAPH PRISM PAD version 8.0.2 was used to compute the results. Statistical analysis was performed using Student's *t*-test with Bonferroni correction for multiple comparisons compared to standard drug. Observations were expressed as values of the mean  $\pm$  SD for each group. The level of statistical significance was set at \*p < 0.05, \*\*p < 0.01, \*\*p < 0.001.

#### **Authors contribution**

The manuscript was written with input from all authors. All authors have approved the final version of the text.

#### CRediT authorship contribution statement

A.C. Kumar: Writing – original draft, Methodology, Investigation, Conceptualization. Madalambika: Methodology, Investigation. P.M. Bharathkumar: Methodology, Investigation. Priyanka R. Patil: Writing – review & editing, Validation, Data curation. J. Rangaswamy: Writing – review & editing, Validation, Data curation. Ramith Ramu: Validation, Software, Investigation, Formal analysis. K.B. Vilas Gowda: Visualization, Validation, Methodology. Nagaraja Naik: Writing – review & editing, Supervision, Investigation, Conceptualization.

#### Declaration of competing interest

The authors declare that they have no known competing financial interests or personal relationships that could have appeared to influence the work reported in this paper.

#### Acknowledgments

The authors gratefully acknowledge the University of Mysore for providing the necessary facilities. A. C. K would like to thank SC & ST Special Cell, University of Mysore (UOM Order No. VG4/4/2020-21 Dated: 08.02.2021/1524) for their financial support for the present work.

#### Appendix A. Supplementary data

Supplementary data to this article can be found online at https://doi.org/10.1016/j.bmc.2025.118425.

#### Data availability

No data was used for the research described in the article.

#### References

- Romo JA, Kumamoto CA. On Commensalism of Candida J Fungi. 2020;6:16. https://doi.org/10.3390/jof6010016.
- Rania H, Soliman Samesh SM, Abrar IA, et al. Design and synthesis of new drugs inhibitors of *Candida albicans* hyphae and biofilm formation by upregulating the expression of TUP1 transcription repressor gene. *Eur J Pharm Sci.* 2020;148, 105327. https://doi.org/10.1016/j.ejps.2020.105327.

- Doblin S, Yasser MT, Ahamd EO, Ishla OA. Resistance of *Candida albicans* biofilms to drugs and the host immune system. *Jundishapur J Microbiol*. 2016;9, e37385. https://doi.org/10.5812/jjm.37385.
- Faria DR, Melo RC, Arita GS, et al. Fungicidal activity of a safe 1,3,4-oxadiazole derivative against *Candida albicans*. *Pathogens*. 2021;10(3):314. https://doi.org/ 10.3390/pathogens10030314.
- Geffers C, Gastmeier P. Nosocomial infections and multidrug-resistant organisms in Germany: epidemiological data from KISS. *Dtsch Arztebl Int.* 2011;108:87–93. https://doi.org/10.3238/arztebl.2011.0087.
- Wenzel RP, Gennings C. Bloodstream infections due to Candida species in the intensive care unit: identifying especially high-risk patients to determine prevention strategies. Clin Infect Dis. 2005;4:S389–S393. https://doi.org/10.1086/430923.
- Dadar M, Tiwari R, Karthik K, Chakraborty S, Shahali Y, Dhama K. Candida albicansbiology, molecular characterization, pathogenicity, and advances in diagnosis and control – an update. Microb Pathog. 2018;117:128–138. https://doi.org/10.1016/j. micpath.2018.02.028.
- Kubinski K, Masiyk M, Janeczko M, et al. Metallacarborane derivatives as innovative anti-Candida albicans agents. J Med Chem. 2022;65:13935–13945. https://doi.org/ 10.1021/acs.jmedchem.2c01167.
- Garzon MG, Gutierrez Castañeda LD, Gil C, et al. Inhibition of the filamentation of Candida albicans by Borojoa patinoi silver nanoparticles. SN Appl Sci. 2021;3:195. https://doi.org/10.1007/s42452-020-04103-0.
- Kumamoto CA. Candida biofilms. Curr Opin Microbiol. 2002;5:608. https://doi.org/ 10.1016/S1369-5274(02)00371-5.
- Patil RH, Kalam Khan FA, Jadhav K, et al. Fungal biofilm inhibition by piperazinesulphonamide linked Schiff bases: design, synthesis, and biological evaluation. Arch Pharm Chem Life Sci. 2018, e1700354. https://doi.org/10.1002/ardp.201700354.
- Seddiki SM, Boucherit-Otmani Z, Boucherit K, Kunkel D. Fungal infectivities of implanted catheters due to Candida sp. Biofilms formation and resistance. J Mycol Médicale. 2015;25:130–135. https://doi.org/10.1016/j.mycmed.2015.03.003.
- Tang N, Yuan S, Luo Y, et al. Nanoparticle-based photodynamic inhibition of Candida albicans biofilms with interfering quorum sensing. ACS omega. 2023;17: 4357–4368. https://doi.org/10.1021/acsomega.2c07740.
- Argimon S, Wishart JA, Leng R, et al. Developmental regulation of an adhesin gene during cellular morphogenesis in the fungal pathogen Candida albicans. *Eukaryot Cell*. 2007;6(4):682–692. https://doi.org/10.1128/ec.00340-06.
- Fan Y, He H, Dong Y, Pan H. Hyphae-specific genes HGC1, ALS3, HWP1, and ECE1 and relevant signaling pathways in Candida albicans. *Mycopathologia*. 2013;176(5): 329–335. https://doi.org/10.1007/s11046-013-9684-6.
- Kim H, Hwang JY, Chung B, et al. 2-Alkyl-4-hydroxyquinolines from a marinederived Streptomyces sp. inhibit hyphal growth induction in Candida albicans. *Marine Drugs*. 2019;17(2):133. https://doi.org/10.3390/md17020133.
- Kornitzer D. Regulation of Candida albicans hyphal morphogenesis by endogenous signals. J of Fungi. 2019;5(1):21. https://doi.org/10.3390/jof5010021.
- Norouzi N, Alizadeh F, Khodavandi A, Jahangiri M. Antifungal activity of menthol alone and in combination on growth inhibition and biofilm formation of Candida albicans. J Herb Med. 2021;29, 100495. https://doi.org/10.1016/j. hermed 2021 100495
- Chen HF, Lan CY. Role of SFP1 in the regulation of Candida albicans biofilm formation. *PLoS One*. 2015;10(6), e0129903. https://doi.org/10.1371/journal. pone.0129003
- Marc G, Araniciu C, Oniga SD, et al. New N-(oxazolylmethyl)-thiazolidinedione active against Candida albicans biofilm: potential Als proteins inhibitors. *Molecules*. 2018;23(10):2522. https://doi.org/10.3390/molecules23102522.
- Lee Y, Puumala E, Robbins N, Cowen LE. Antifungal drug resistance: molecular mechanisms in Candida albicans and beyond. *Chem Rev.* 2020;121(6):3390–3411. https://doi.org/10.1021/acs.chemrev.0c00199.
- Sari S, Kart D, Oztürk N, et al. Discovery of new azoles with potent activity against Candida spp. and Candida albicans biofilms through virtual screening. Eur J Med Chem. 2019;179:634–648. https://doi.org/10.1016/j.ejmech.2019.06.083.
- Prasad R, Shah AH, Rawal MK. Antifungals: mechanism of action and drug resistance. Yeast Membrane Transport. 2016;1:327–349. https://doi.org/10.1007/ 978.3.319.25304-6.14
- Wani MY, Ahmad A, Aqlan FM, Al-Bogami AS. Azole based acetohydrazide derivatives of cinnamaldehyde target and kill Candida albicans by causing cellular apoptosis. ACS Med Chem Lett. 2020;11(4):566–574. https://doi.org/10.1021/ acsmedchemlett.0c00030.
- Hu C, Xu Z, Huang Z, Wang R, Zhang Y, Mao Z. Synthesis and antifungal evaluation of new azole derivatives against Candida albicans. ACS Med Chem Lett. 2023;14(10): 1448–1454. https://doi.org/10.1021/acsmedchemlett.3c00361.
- Kelly SL, Lamb DC, Kelly DE, et al. Resistance to fluconazole and cross-resistance to amphotericin B in Candida albicans from AIDS patients caused by defective sterol Δ5, 6-desaturation. FEBS Lett. 1997;400(1):80–82. https://doi.org/10.1016/S0014-5793(96)01360-9
- Khan MS, Malik A, Ahmad I. Anti-candidal activity of essential oils alone and in combination with amphotericin B or fluconazole against multi-drug resistant isolates of Candida albicans. *Med Mycol*. 2012;50(1):33–42. https://doi.org/ 10.3109/13693786 2011 583800
- Tahlan S, Singh S, Dey H, Kaira M, Pandey KC. Recent research Frontiers of heterocycles as antifungal agents: insights from the past five years. Eur J Med Chem. 2025;23, 117801. https://doi.org/10.1016/j.ejmech.2025.117801.
- Sahin G, Palaska E, Ekizoglu M, Ozalp M. Synthesis and antimicrobial activity of some 1, 3, 4-oxadiazole derivatives. Il Farmaco. 2002;57(7):539–542. https://doi. org/10.1016/S0014-827X(02)01245-4.
- Rollas S, Guniz Kucukguzel S. Biological activities of hydrazone derivatives. *Molecules*. 2007;12(8):1910–1939. https://doi.org/10.3390/12081910.

- Salahuddin Mazumder A, Yar MS, Mazumder R, Chakraborthy GS, Ahsan MJ, Rahman MU. Updates on synthesis and biological activities of 1, 3, 4-oxadiazole: a review. Synth Commun. 2017;47(20):1805–1847. https://doi.org/10.1080/ 00397911.2017.1360911.
- 32. Kioshima ES, Svidzinski TIE, Bonfim-Mendonça PS, et al. Composição farmacêutica baseada em compostos 1,3,4-oxadiazólicos e seu uso na preparação de medicamentos para tratamento de infecções sistêmicas. *Brazil patent BR*. 2018;10, 009020 8. 03 May 2018.
- Rodrigues-Vendramini FA, Faria DR, Arita GS, et al. Antifungal activity of two oxadiazole compounds for the paracoccidioidomycosis treatment. *PLoS Negl Trop Dis.* 2019;13(6), e0007441. https://doi.org/10.1371/journal.pntd.0007441.
- Capoci IR, Sakita KM, Faria DR, et al. Two new 1, 3, 4-oxadiazoles with effective antifungal activity against Candida albicans. Front Microbiol. 2019;10:2130. https://doi.org/10.3389/fmicb.2019.02130.
- Faria DR, Sakita KM, Capoci IR, et al. Promising antifungal activity of new oxadiazole against Candida krusei. *PLoS One*. 2020;15(1), e0227876. https://doi. org/10.1371/journal.pone.0227876.
- Nasr AZ, Farahat A, Zein MA, Abdelrehim ES. Synthesis and antimicrobial activity of 1, 3, 4-Oxadiazoline, 1, 3-thiazolidine, and 1, 2, 4-triazoline double-tailed Acyclo C-nucleosides. ACS omega. 2022;7(20):16884–16894. https://doi.org/10.1021/acsomega.1c06339.
- Mehandi R, Twala C, Ahmedi S, et al. 1, 3, 4-oxadiazole derivatives: synthesis, characterization, antifungal activity, DNA binding investigations, TD-DFT calculations, and molecular modelling. *J Biomol Struct Dyn.* 2025;43(4):1723–1755. https://doi.org/10.1080/07391102.2023.2292796.
- Wani MY, Ahmad A, Shiekh RA, Al-Ghamdi KJ, Sobral AJ. Imidazole clubbed 1, 3, 4oxadiazole derivatives as potential antifungal agents. *Bioorg Med Chem.* 2015;23
  (15):4172–4180. https://doi.org/10.1016/j.bmc.2015.06.053.
- Kumar AC, Rangaswamy J, BharathKumar PM, Patil PR, Salavadi M, Naik N. Novel
  1, 3, 4-oxadiazole-2-thiol derivatives: unlocking the therapeutic potential as antiinflammatory and anticancer agents. *JMol Struc*. 2024;1315, 138749. https://doi.
  org/10.1016/j.molstruc.2024.138749.
- Lieberman S, Enig MG, Preuss HG. A review of monolaurin and lauric acid: natural virucidal and bactericidal agents. Alternative & Complementary Therapies. 2006;12 (6):310–314. https://doi.org/10.1089/act.2006.12.310.
- Ameena M, Meignana A, Karthikeyan R, Rajeshkumar S. Biomedical applications of lauric acid: a narrative review. *Cureus*. 2024;16:6. https://doi.org/10.7759/ cureus.62770.
- Yıldırım A, Oztürk SE. Synthesis and surface characterization studies of polyetherlinked symmetric higher sulfanyl-1, 3, 4-oxadiazoles. *Phosphorus Sulfur Silicon Relat Elem*. 2015;190(9):1535–1550. https://doi.org/10.1080/10426507.2014.999067.
- Gandhi B, Jhansi M, Deshpande SS, Vinay T, Misra S, Kaki SS. Design, synthesis and biological activity of novel oxadiazole containing monoacylglycerols as potential bioactive lipids. *J Mol Strc.* 2023;1284, 135424. https://doi.org/10.1016/j. molstruc.2023.135424.
- Neto V, Voisin A, Héroguez V, Grelier S, Coma V. Influence of the variation of the alkyl chain length of N-alkyl-β-d-glycosylamine derivatives on antifungal properties. *J Agric Food Chem.* 2012;60(42):10516–10522. https://doi.org/10.1021/jf3015798.
- Pathan SK, Shelar A, Deshmukh S, et al. Exploring antibiofilm potential of some new imidazole analogs against C. Albicans: synthesis, antifungal activity, molecular

- docking and molecular dynamics studies. *J Biomol Struct Dyn.* 2025;43(6): 3099–3115. https://doi.org/10.1080/07391102.2023.2296604.
- Wu D, Chen Q, Chen X, Han F, Chen Z, Wang Y. The blood–brain barrier: structure, regulation and drug delivery. Signal Transduct Target Ther. 2023;8(1):217. https://doi.org/10.1038/s41392-023-01481-w.
- CLSI. Method for antifungal disk diffusion susceptibility testing of yeasts, approved guideline. CLSI Document M44-a. CLSI, 940 West Valley Road, Suite 1400, Wayne, Pennsylvania. USA 19087–1898. 2004. https://doi.org/10.1080/ 07391102.2023.2296604.
- Salari S, Almani Ghasemi Nejad, P.. Antifungal effects of lactobacillus acidophilus and lactobacillus plantarum against different oral Candida species isolated from HIV/AIDS patients: an in vitro study. *J Oral Microbiol*. 2020;12(1), 1769386. https://doi.org/10.1080/20002297.2020.1769386.
- Aarti C, Khusro A, Varghese R, et al. In vitro investigation on probiotic, anti-Candida, and antibiofilm properties of lactobacillus pentosus strain LAP1. Arch Oral Biol. 2018;89:99–106. https://doi.org/10.1016/j.archoralbio.2018.02.014.
- Wang S, Wang Q, Yang E, Yan L, Li T, Zhuang H. Antimicrobial compounds produced by vaginal lactobacillus crispatus are able to strongly inhibit Candida albicans growth, hyphal formation and regulate virulence-related gene expressions. *Front Microbiol.* 2017;8, 258246. https://doi.org/10.3389/fmicb.2017.00564.
- Rossoni RD, De Barros PP, Mendonça ID, et al. The postbiotic activity of lactobacillus paracasei 28.4 against Candida auris. Front Cell Infect Microbiol. 2020; 10:397. https://doi.org/10.3389/fcimb.2020.00397.
- Poon Y, Hui M. Inhibitory effect of lactobacilli supernatants on biofilm and filamentation of Candida albicans, Candida tropicalis, and Candida parapsilosis. Front Microbiol. 2023;14, 1105949. https://doi.org/10.3389/fmicb.2023.1105949.
- Maione A, Imparato M, Buonanno A, et al. Anti-biofilm activity of phenyllactic acid against clinical isolates of fluconazole-resistant Candida albicans. *J Fungi.* 2023;9(3): 355. https://doi.org/10.3390/jof9030355.
- Turecka K, Chylewska A, Kawiak A, Waleron KF. Antifungal activity and mechanism of action of the co (III) coordination complexes with diamine chelate ligands against reference and clinical strains of Candida spp. Front Microbiol. 2018;9:1594. https:// doi.org/10.3389/fmicb.2018.01594.
- Barbosa JO, Rossoni RD, Vilela SF, et al. Streptococcus mutans can modulate biofilm formation and attenuate the virulence of Candida albicans. *PLoS One.* 2016;11(3), e0150457. https://doi.org/10.1371/journal.pone.0150457.
- Gundogdu S, Duran HE, Arslan M, Cetinkaya BD, Turkes C. Fluorenyl-phthalimide hybrids as potent aldose reductase inhibitors with selective anticancer activity: rational design, synthesis, and molecular insights. *Bioorg Chem.* 2025, 108689. https://doi.org/10.1016/j.bioorg.2025.108689.
- Zognjani B, Nixha AR, Duran HE, et al. N-substituted phthalimide-carboxylic acid hybrids as dual-targeted aldose reductase inhibitors: synthesis, mechanistic insights, and cancer-relevant profiling. *Bioorg Chem.* 2025, 108788. https://doi.org/10.1016/ ibioorg.2025.108788.
- Gulec O, Duran HE, Arslan M, Yıldıztekin G, Ece A, Turkes C. Chalcone-inspired indole, carbazole, and phenothiazine hybrids as potent aldose reductase inhibitors with selective anticancer potential: rational design, synthesis, and multi-level characterization. *Bioorg. Chem.* 2025;164, 108861. https://doi.org/10.1016/j. bioorg.2025.108861.